

Aus der Klinik und Poliklinik für Anästhesiologie
der Universität Würzburg

Direktor: Prof. Dr. med. Dr. h.c. N. Roewer

New players in neuropathic pain? microRNA expression in dorsal root
ganglia and differential transcriptional profiling in primary sensory
neurons

Inaugural-Dissertation
zur Erlangung der Doktorwürde der
Medizinischen Fakultät
der
Julius-Maximilians-Universität Würzburg
vorgelegt von
Ann-Kristin Reinhold
aus Münster

Würzburg, Juni 2016



Referentin: Prof. Dr. med. Heike Rittner

Koreferentin: Prof. Dr. med. Claudia Sommer

Dekan: Prof. Dr. Matthias Frosch

Tag der mündlichen Prüfung: 28.06.2016

Die Promovendin ist Ärztin

Meinen Eltern gewidmet

Table of contents

1	Introduction	1
1.1	Pain and Nociception	1
1.2	Neuropathic Pain	3
1.2.1	Aetiologies & Symptoms	
1.2.2	Molecular Mechanisms	
1.2.2.1	Ion Channels	
1.2.2.2	Immune and Glial Modulations	
1.2.2.3	Central Mechanisms	
1.2.3	Animal Models of Neuropathic Pain	
1.2.4	Epidemiology and Treatments	
1.3	MicroRNAs	8
1.3.1	Biogenesis	
1.3.2	Working Principles	
1.3.3	miRNA Target Prediction	
1.3.4	miRNAs in Medicine	
1.4	MicroRNAs in Pain	11
1.5	Neuronal Tracing	12
2	Objectives	14
3	Methods	15
3.1	Animals	15
3.2	Tissue	15
3.2.1	Surgery	
3.2.2	Neuronal Staining	
3.2.3	Tissue Collection	
3.2.4	RNA Extraction	
3.3	Assessment of Surgical Effect	17
3.4	MicroRNA Assay	18
3.5	qRT-PCR	19
3.6	Histology	20
3.6.1	<i>In situ</i> Hybridization	
3.6.2	Immunohistochemistry	
3.7	Neuron-Specific RNA Analysis	22
3.7.1	Cell Isolation and FACS	
3.7.2	RNA Extraction and Analysis	
3.8	Bioinformatics	23
3.8.1	<i>SylArray</i>	
3.8.2	<i>MirAct</i>	
3.8.3	<i>myMIR</i>	
3.9	Data Processing	24
3.9.1	Data Calculation	
3.9.2	Data Analysis	
4	Results	26
4.1	CCI Produces a Neuropathy-Specific Response	26
4.2	MicroRNAs are Regulated in CCI	27
4.2.1	Increase in microRNA Regulation over Time	
4.2.2	Predominantly Downregulation of microRNAs	

4.3	Validation of Regulation Patterns for Selected microRNAs	29
4.3.1	miR-183	
4.3.2	miR-137	
4.3.3	miR-124	
4.3.4	miR-505	
4.3.5	miR-27b	
4.4	<i>In Silico</i> Target Prediction for Selected microRNAs	32
4.4.1	miR-183	
4.4.2	miR-137	
4.5	Localization of miR-183 and -137 in DRG	34
4.6	Neuronal Tracing Allows Distinction between Damaged And Intact Neurons	36
4.7	Distinct mRNA Expression Patterns in Damaged vs Intact DRG Neurons after CCI	38
4.7.1	Class Comparison of mRNA Regulation	
4.7.2	Differentially Regulated Genes after CCI	
4.7.2.1	Damaged vs. Contralateral DRG Neurons	
4.7.2.2	Damaged vs. Adjacent Spared DRG Neurons	
4.7.2.3	Regulated Ion Channels	
4.7.2.4	Regulated Peptides	
4.7.2.5	Regulation of microRNA Top Targets	
4.8	<i>In Silico</i> Deduction of microRNA Involvement after CCI	45
4.8.1	<i>SylArray</i> Analysis	
4.8.2	<i>MirAct</i> Analysis	
5	Discussion	52
5.1	MicroRNAs in Neuropathic Pain	52
5.1.1	Time Course of microRNA Expression in DRG after CCI	
5.1.2	MicroRNA Profiling in Contralateral DRG	
5.2	MiRNAs Potentially Involved In Neuropathic Pain	52
5.2.1	miR-183 in Various States of Pain	
5.2.2	miR-137 in Sensory Neurons and its Role in Pain	
5.2.3	miR-124 in Pain – Neuronal or Immune Origin?	
5.2.4	miR-505 and miR-27b	
5.2.5	Further microRNAs Described in Neuropathic Pain	
5.3	Divergent Results in microRNA Profiling	57
5.4	Neuron-Specific Approach	58
5.4.1	Advantages of Cell Type- and Damage-Specific Approach	
5.4.2	mRNA Regulation in Damaged Neurons	
5.4.2.1	Global Findings	
5.4.2.2	Regulation of Genes Described in Neuropathic Pain	
5.4.2.3	Novel Regulated Genes	
5.4.3	Bioinformatical Inference on Potential microRNA Contribution	
5.5	Outlook	65
5.5.1	Validation of miR-183 and -137 in Neuropathic Pain	
5.5.2	Further Characterisation of Specific Genes in Neuropathic Pain	
5.5.3	Cell Type-Specific Expression Analysis	
6	Summary/Zusammenfassung	68
6.1	Summary	68

6.2 Zusammenfassung.....	70
7 Bibliography.....	72
8 List of Figures and Tables.....	78
9 Abbreviations.....	79

1 Introduction

1.1 Pain and Nociception

Pain is a concept commonly used to describe unpleasant states of the most diverse kind. Accordingly, in 1979, the International Association for the Study of Pain (IASP) defined pain very broadly as “... an unpleasant sensory and emotional experience associated with actual or potential tissue damage, or described in terms of such damage” (cf. Bonica, 1979). Besides the physiological transduction of stimuli, it thus requires additional cognitive and emotional processing and is often even used as a concept void of any immediate physical experience.

In contrast to the culturally and psychologically connoted concept of pain, the sheer physiological processes are referred to as nociception. It primarily serves as a warning device against potentially noxious stimuli, be they thermal (e.g., a hot plate or an ice bucket), mechanical (a harsh squeeze), or chemical (hot chilli pepper).

In mammals, the detection of such stimuli is carried out by specific receptors, so-called nociceptors, of the peripheral nervous system (PNS) which transform the stimulus into an electric impulse (*transduction*). In contrast to encapsulated detectors of innocuous tactile stimuli, nociceptors are bare nerve endings in cutaneous as well as visceral tissue. The cell bodies of these pseudo-unipolar primary afferent neurons are located in trigeminal (TG) or dorsal root ganglia (DRG) and innervate head and body, respectively. Whereas TG are restricted to cranial nerve fibres, DRG are conglomerates of several thousand¹ sensory nerve bodies (somata), located in the dorsal root of the spinal nerves and thus responsible for segmental body innervation. From the DRG, the primary nociceptive neurons enter the spinal cord through the ipsilateral dorsal horn, where they connect to the central nervous system (CNS) (*transmission*). Secondary neurons cross to the contralateral side via the anterior commissure, and ascend in the lateral spinothalamic tract to the lateral thalamic nuclei. From there, they project towards the primary sensory cortex (*perception*), but also to subcortical structures like the limbic system where signals are further processed. Descending pathways from the cerebrum, in turn, regulate nociception (*modulation*) (**Fig. 1**, for details see Schaible & Richter, 2004).

¹ Lawson (1979) estimates 6,000 neurons in L3 DRG of adult mice; Shi et al. (2001) counted 12,000 in murine L5 DRG.

Nociceptors contain two classes of neural fibres that differ in the nociceptive character

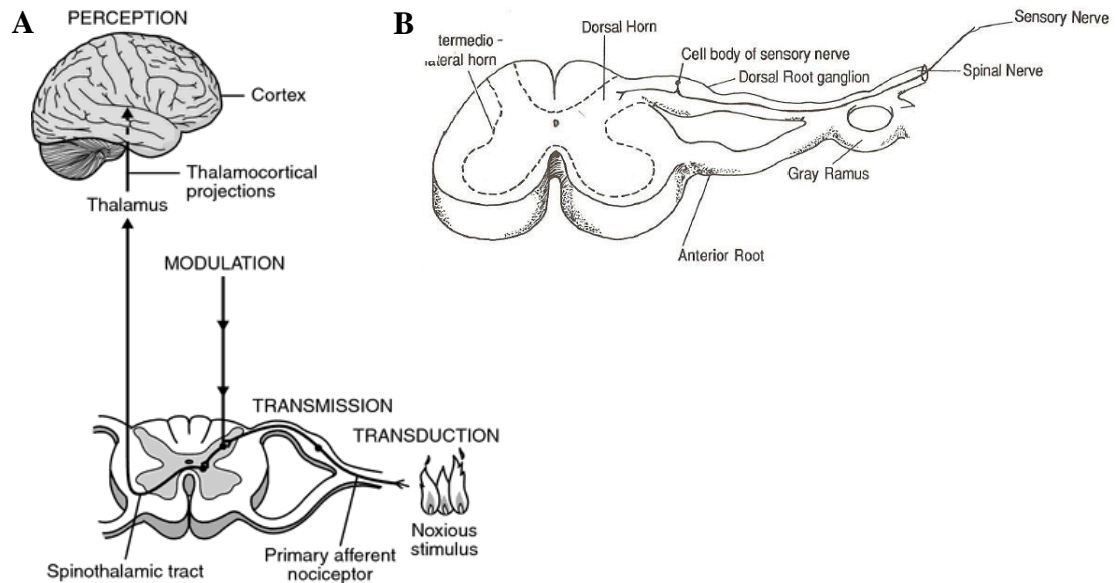


Figure 1: Principles of nociception

A: Principal nociceptive pathways. **B:** Topological anatomy of the peripheral sensory nervous system (from Ferrante & VadeBoncoeur, 1993).

elicited and in the velocity by which the stimulus is conducted. A δ fibres are thinly myelinated, have a diameter of 30-40 μm , and transport signals at a velocity of about 1-10 m/s, whereas C fibres are unmyelinated, thinner (<30 μm) and, with a conduction rate of <1 m/s, are considerably slower (Erlanger & Gasser, 1930; reviewed in Whitwam, 1976). All these classes lack heavy neurofilaments like neurofilament 200 (NF200) which distinguishes them from big and medium-sized myelinated A β fibres.

C fibres can each be further classified by their molecular properties: One subset, so-called “peptidergic” fibres, expresses pro-inflammatory peptides, such as substance P and calcitonin gene-related peptide (CGRP). A second, “non-peptidergic” group does not express such peptides but shows other properties, e.g., binding sites for lectin IB4. Furthermore, these sets differ in affinity to neurotrophic factors, electrophysiological properties, and spatial distribution (Boucher & McMahon, 2001; Stucky & Lewin, 1999; Caterina & Julius, 1997).

1.2 Neuropathic Pain

In contrast to its function as a warning device, pain can also be evoked without the presence of noxious stimuli. As this pain experience is due to neuronal pathology, it is referred to as “neuropathic pain”. According to the IASP, neuropathic pain is “arising as direct consequence of a lesion or disease affecting the somatosensory system.” (Treede et al., 2008). This broad definition reflects the diversity of underlying aetiologies and locations as well as symptoms.

1.2.1 Aetiologies and Symptoms

Causes of neuropathic pain are very diverse: They include benign as well as paraneoplastic syndromes; pain may be caused by chronic diseases as well as by trauma; it can be located and evoked in the peripheral as well as in the central nervous system. Moreover, one medical condition can cause several neuropathic mechanisms: Diabetic neuropathy, for example, is caused by direct nerve damage due to free radicals as well as secondary damage caused by angiopathy (cf. table 1 for examples).

	<i>Peripheral Nervous System</i>	<i>Central Nervous System</i>
<i>Autoimmune</i>	polyarthritis nodosa	multiple sclerosis
<i>Infectious</i>	VZV, HIV, neuroborreliosis	HIV, tuberculosis, syphilitic myelitis
<i>Metabolic/toxic</i>	diabetes mellitus, hypothyroidism, alcohol, pharmacotherapy	myelosis funicularis
<i>Vascular</i>	microangiopathy, trigeminal neuralgia	brain infarction, arterio-venous malformation
<i>Congenital</i>	hereditary neuropathies (Charcot-Marie-Tooth)	syringomyelia, dysraphism
<i>Mechanic/traumatic</i>	phantom limb syndrome, entrapment syndromes	spinal cord injury, disc herniation
<i>Malignant</i>	plasmocytoma, paraneoplastic syndrome	primary CNS tumours, metastases

Table 1: Exemplary aetiologies of central and peripheral neuropathic pain (cf. Baron, 2006).

Moreover, neuropathic pain can manifest itself in different ways: Features include not

only diverse, but also opposed, “positive” and “negative” symptoms: paraesthesia as well as hypaesthesia, allodynia as well as hyperalgesia (Woolf & Mannion, 1999). The pain may be described as “burning”, “itching”, or “numb”; it may be constant or paroxysmal. It is for these incongruities in aetiologies and symptoms that diagnosis often proves difficult and treatment outcome is moderate. An attempt to classify and treat neuropathic pain based on symptoms rather than aetiologies (e.g. Baron, 2006; Rolke et al., 2006) is still under debate.

1.2.2 Molecular Mechanisms

Given such diversity in aetiologies and manifestations, also cellular and molecular mechanisms of neuropathic pain are complex and may vary considerably. However, certain features have been identified that are central to initiation and maintenance of neuropathic pain.

Relevant modifications occur at several locations: At the site of injury as well as in primary sensory neuron somata, in damaged as well as in adjacent intact neurons, in the CNS as well as in the PNS, in neurons as well as in immune or glial cells (Campbell & Meyer, 2006).

At the site of injury, due to neuronal damage and Wallerian degeneration, pro-inflammatory mediators are released, such as prostaglandin E₂ (PGE₂), bradykinin, reactive oxygen species (ROS), nitric oxide (NO), protons, histamine, neurotrophins, interleukins (IL-1), tumour necrosis factor α (TNF- α), cytokines, serotonin (HT-5), glutamate, or adenosintriphosphate (ATP), a mix often referred to as “inflammatory soup”. Regulatory mechanisms include both ionotropic and metabotropic effects (e.g. activation of tyrosine kinase receptors by neurotrophins). A central role play neuropeptides such as substance P, neuropeptide Y, CGRP, cholecystokinin, galanin, and neurotensin: These peptides not only alter neuronal excitability but also account for long-lasting effects as they may influence gene expression and synaptogenesis by activating G-protein-coupled receptors (GPCR). They show complex regulation in neuropathic pain (Ji & Strichartz, 2004).

1.2.2.1 Ion Channels

A central feature of neuropathic pain is the altered excitability of neurons, i.e. a change in membrane properties. This is mainly achieved by modifications in membrane ion

channel expression. Prominent examples are voltage-gated sodium channels: Whereas slow-inactivating tetrodotoxin (TTX)-resistant channels Nav1.8 and Nav1.9 are downregulated, quick-inactivating TTX-sensitive Nav1.3, physiological only in embryonic DRG, is upregulated. These changes alter membrane properties thus allowing for repetitive bursting discharges (Ekberg & Adams, 2006; Wood et al., 2004). Calcium currents are modified by expression of ionotropic ATP receptor family P2X, Ca_vα2δ1 subunit (upregulation) as well as L- and T-type channels (downregulation) (Ji & Strichartz, 2004). Interestingly, the decrease in the latter causes enhanced excitability as it inhibits Ca²⁺-modulated K⁺ currents. Of K⁺ currents, mostly G protein-activated rectifying potassium channels (GIRK) control resting potential. Other potassium channels include delayed rectifying channels and KCNQ channels. While many K⁺ channels exhibit antinociceptive features (Ocaña et al., 2004), there are reports of downregulation in neuropathic pain (e.g. Rose et al., 2011).

A group of less selective cation channels involved in neuropathic pain are transient receptor potential (TRP) channels, most notably TRPV1 (upregulation), TRPM3, TRPM8, and TRPA1 (downregulation) (Ji & Strichartz, 2004; Staaf et al., 2009; Caspani et al., 2009).

Due to changes in ion channel expression, membrane potentials are altered and damaged axons tend to spontaneously emit action potentials without external stimulus.

This ectopic firing affects not only the site of injury: Also cell bodies in the DRG undergo significant changes as described above (Campbell & Meyer, 2006).

Importantly, the initial “inflammatory soup” and subsequent expression alterations also affect adjacent non-damaged nociceptors (Ji & Strichartz, 2004; Moalem & Tracey, 2005): The milieu at the site of injury can affect their sensitivity and their spontaneous activity. This has been observed mostly for C fibres and goes along with a differential regulation of various genes. Repetitive excitation of neurons causes further long-lasting modifications in gene expression often resulting in again increased excitability. **Figure 2** shows the complex transcriptional regulation of genes in injured and non-injured primary sensory neurons.

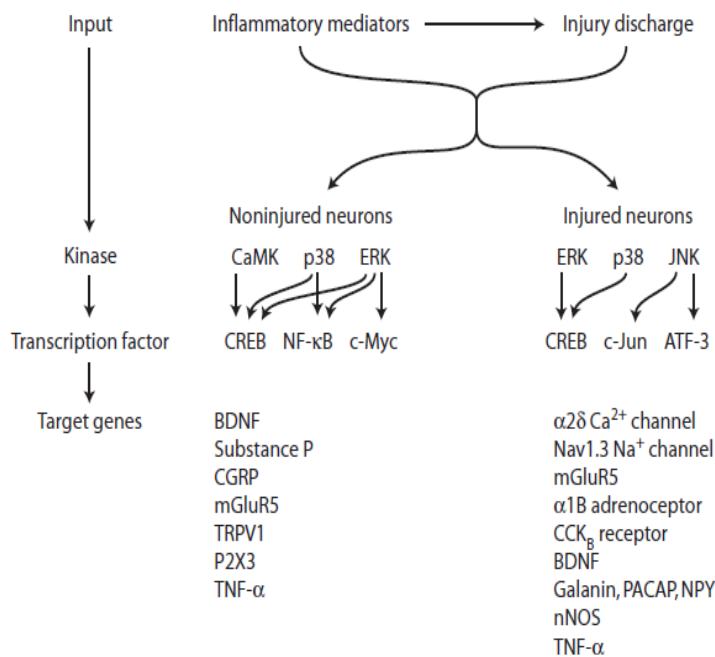


Figure 2: Regulatory pathways in injured and non-injured neurons (from Ji & Strichartz, 2004).

1.2.2.2 Immune and Glial Modulations

One important factor that contributes to enhanced sensitization is the role of non-neuronal cells. Throughout the past years, the relevance of immune cells and glia in the maintenance and perseverance of neuropathic states has become evident. In fact, Scholz & Woolf (2007) assume a “neuropathic triad”: Neuropathic alterations start with the initial inflammatory response described above. Macrophages are activated and recruited by chemokines released from the lesion site. Their activation causes blood-nerve barrier destruction and hyperaemia by matrix metalloproteinases and vasoactive mediators, thus facilitating further infiltration with macrophages, T lymphocytes and mast cells. Furthermore, they enhance post-translational regulation in primary sensory neurons by release of inflammatory mediators like TNF- α and interleukins.

A good example of interaction between neuronal and glial cells is neuregulin, a growth factor on the axonal membrane that acts on Schwann cells. In a first response, it induces demyelination via tyrosine kinase receptor ERBB2, which is later associated with remyelination. In turn, Schwann cells promote further nociceptor sensitization by release of NGF and GDNF, PGE2 and cytokines (reviewed by Scholz & Woolf, 2007; Ohara et al., 2009).

In this context, it is relevant to emphasize that immune and glial cells, in variable proportions, constitute the bulk of DRG cells, only ~15% of all DRG cells are neuronal (Ng et al., 2010). This diversity needs to be considered in the experimental setting and interpretation of results (see chapter 1.5).

1.2.2.3 Central Mechanisms

Furthermore, various modulations occur in the CNS, such as a central sensitization in postsynaptic dorsal horn cells caused by microglia activation and an increased descending responsiveness. As this thesis deals with alterations in the PNS, though, I will not further elaborate on these mechanisms (for further details, see Campbell, 2006).

1.2.3 Animal Models of Neuropathic Pain

In animals, various models have been developed mimicking different forms of neuropathic pain. Among the most frequently used are peripheral nerve injuries in rodents, such as Spinal Nerve Ligation (SNL) or Chronic Constriction Injury (CCI), where spinal or peripheral nerves are being continuously irritated (Kim & Chung, 1992; Bennett & Xie, 1988). In contrast, axotomy models such as Sciatic Nerve Transection (SNT, Wall et al., 1974) emulate a deafferentation rather than neuropathic phenotype. Other non-traumatic models include chemical induction (e.g. streptozotocin for diabetic neuropathy, Jakobsen & Lundbaek, 1976) or *in-vitro* approaches like stress induction by cell isolation (described by Zheng et al., 2007). In this study, the Chronic Constriction Injury model was used as it is well-established in rodents, easy to perform, provides a distinct, well-described phenotype, and is widely accepted as an apt model.

1.2.4 Epidemiology and Treatments

As neuropathic pain imposes severe restrictions on everyday life (Jensen et al., 2007), enormous pressure for therapeutic management exists, all the more as neuropathic pain is a growing medical condition. Due to its association with lifestyle diseases like type 2 diabetes mellitus or with medical treatment (chemotherapy) its prevalence is on the rise: Numbers in literature vary from 1.5% (1998, USA) to 17.9% (2006, Canada) of the population, with an increasing tendency (cf. Bennett, 1998; Toth et al., 2006). This rise is all the more alarming as it represents a heavy economic burden: A survey from 2000

suggested annual costs of \$17,350 per patient in the US, more than three times the costs of matched controls (Berger et al., published 2004)². Yet, despite efforts, adequate treatment still remains difficult: only 40-60% of the patients experience at least partial relief after pharmacological treatment (Dworkin et al., 2007).

Among the most effective drugs are tricyclic antidepressants (re-uptake inhibitors of neurotransmitters), anticonvulsants (esp. Ca_v blockers like Gabapentin), and opioids. Still, success parameters like the number of patients needed to treat (NNT) remain poor (for details, see Attal et al., 2006). One reason is certainly the often only accidental discovery of their beneficence: They consequently represent only a symptomatic approach. Other, targeting approaches include cell and gene therapy (Jain, 2008; Dray, 2008) but are at present still at an experimental stage. Invasive treatments such as microvascular decompression or neuroablation in trigeminal neuralgia can be considered only a final alternative in severe cases (Tronnier & Rasche, 2009).

1.3 MicroRNAs

MicroRNAs (miRNAs) are small (20-23 nucleotides (nt)), single-stranded non-coding RNAs that have been shown to play a crucial role in post-transcriptional gene regulation. They were first described in 1993, for *C. elegans*, by Lee et al. In 2000, Pasquinelli et al. detected analogous RNA molecules in a variety of species, including the human genome, thus indicating a general, conserved principle of gene expression regulation (Pasquinelli et al., 2000). One year later, the term *microRNA* was coined (e.g., Lagos-Quintana et al., 2001). Since then, miRNAs have been revealed as an important regulative factor in gene expression and have elicited intense research. By now, the number of miRNAs identified in genomes of animals, plants, fungi, and viruses amounts to thousands, many of them suggesting an ancient well-conserved role in gene regulation. For mice, more than 800 miRNAs are currently known (<http://www.mirbase.org/>, retrieved last on Aug 18, 2013).

1.3.1 Biogenesis

MiRNA in the DNA may be located inter- or intragenetically, i.e. between coding genes

2 This number derives from frequent medical consultations, expensive treatment and frequent co-morbidities like reactive depression. Moreover, as neuropathic pain is often related with work impairment, real costs are considered much higher.

or within, in the latter case mostly in introns. By now, biogenesis has been extensively researched (**Fig. 3**): After the primary nuclear transcript (*pri-miRNA*) is produced, part of it folds to a ~60nt imperfect stem-loop hairpin structure, called *pre-miRNA*. The *pre-miRNA* is excised by a nuclear protein complex consisting of endoribonuclease *Drosha* and protein *DGCR8*, followed by transfer to the cytoplasm by cargo transporter *Exportin 5*. There, the *pre-miRNA* is processed by *Dicer*, an RNase similar to *Drosha*,

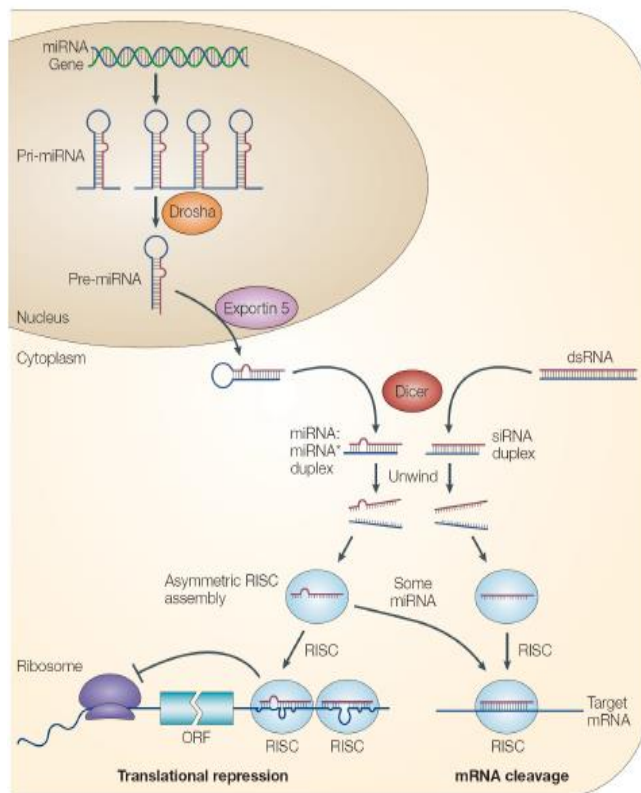


Figure 3: Principles of miRNA biogenesis and action (from He & Hannon, 2004).

which degrades the loop structure. After the remaining duplex miRNA is unwound, one “guide” miRNA strand is loaded into an RNA-induced silencing (*RISC*) or microRNA ribonucleoprotein complex (*miRNP*) whereas the “passenger” strand is degraded (Guarnieri & DiLeone, 2008).

1.3.2 Working Principles

The exact molecular mechanisms of miRNA-involving post-transcriptional regulation are still subject to debate but certain features are regarded as central:

In general, it interacts with the messenger RNA (mRNA) of a gene before translation.

Two basic principles of miRNA-mRNA interaction can be distinguished: mRNA cleavage and translational repression. In plants, the *RISC* containing the miRNA recognizes a stretch of complementary bases in the 3'-untranslated region (UTR) of a target mRNA and induces mRNA cleavage by argonaute proteins with endonuclease activity (Ago). In metazoa, in contrast, miRNA and 3'UTR of the target mRNA most commonly share only partial complementarity, displaying a) contiguous Watson-Crick pairing in the so-called 5' proximal seed region (~nt 2-8), responsible for target recognition and b) incomplete homology in the central part (nt 10-11) which precludes endonucleolytic cleavage of the target mRNA by Agos (Pillai et al., 2007). Instead, the miRNP:mRNA complex is translocated to small cytoplasmic foci called *p-bodies* (processing bodies). These contain enzymes responsible for mRNA degradation but can also serve as “temporary storage sites” from where mRNAs can re-enter translation (Pillai et al., 2007; Kulkarni et al., 2010).³ Although most miRNA research so far has focused on repressive regulation, further mechanisms including gene-enhancing instead of silencing (Vasudevan et al., 2007) are being discussed.

1.3.3 miRNA Target Prediction

Analyses estimate that miRNAs regulate about 30% of the human genome (Lewis et al., 2005). Still, target prediction results challenging due to several factors: First of all, the small size of 20-23nt and a relevant seed sequence of merely ~7nt impede discrimination between random sequence correlation and functional relevance. Second, miRNAs seem to act pleiotropically: It is estimated that up to 200 genes can be targeted by a single miRNA (Krützfeldt et al., 2005). At the same time, genes may be regulated by different miRNAs independently: Such redundancy indicates the possibility of combinatorial action to maximize inhibitory effects. Moreover, as the field is rather young, only few validated targets exist that might serve as model for further predictions. Still, the major obstacle lies in the imperfect homology between miRNA and target required. Several computational approaches have been developed, based on factors that determine miRNA:mRNA binding, such as between-species conservation, stringency of seed pairing, site number, site type, thermodynamical considerations, or predicted

³ Besides the effect on translation initiation, other models propose miRNA involvement in later stages of translation (cf. Peterson et al., 2006, for details).

pairing stability. (for details, see Bartel, 2009). Still, established databases like *miRANDA*, *TargetScan* or *PicTar* suggest up to 1,000 potential target genes for a single miRNA with sometimes surprisingly diverging results. Recently developed databases like *myMIR* aim at integrating these different approaches. A rather novel bioinformatical approach is the deduction of miRNA involvement from sequence comparison to differentially regulated genes (e.g. *SylArray*, *mirAct*, see chapter 3.8).

1.3.4 miRNAs in Medicine

By now, miRNAs have been described in many fields, especially in developmental pathways, carcinogenesis and immunological processes. Despite its rather recent discovery, miRNA dysregulation has been suggested as pathomechanism for a number of clinical conditions. Examples include neoplasia like ovarian cancer (Iorio et al., 2007), congenital defects such as polycystic kidney disease (Chu & Friedman, 2008), or viral infects like Hepatitis C (van der Ree, 2014) but also conditions not primarily related to developmental or differentiation disorders: MiR-133, for example, is discussed as potential serum biomarker for myocardial infarction (Cheng et al., 2014). Besides its putative role as diagnostic tool, studies also aim at using miRNAs as therapeutic targets or agents (e.g. Baek et al., 2013, on miR-122 in hepatitis C). As yet, however, attempts have been only experimental.

1.4 MicroRNAs in Pain

Despite the enthusiasm about miRNAs, surprisingly little has been published on their role in pain and nociception. In fact, when I started this project, only one paper had been released concerning peripheral pain, by Bai et al. (2007) who reported differential expression of seven miRNAs in TG after inflammatory muscle pain. They described a downregulation in miR-10a, -29a, -98, -99a, -124a, -134, and -183 by up to 80% within min. The effect lasted between 1 and 4 d and in some cases even resulted in later over-expression (Bai et al., 2007).

By now, several studies have been published on miRNA in the PNS and pain. The principle of miRNAs in inflammatory pain has been proven by creating a conditional Dicer knockout mouse that showed diminished pain response to inflammatory mediators (Zhao et al., 2010). Aldrich et al. (2009) described a downregulation of miR-

182/-183/-96 in DRG following SNL. Yu et al. (2011) reported differential regulation of miR-21, miR-221 (upregulation), miR-500 and miR-551b (downregulation) after sciatic nerve transection (i.e. deafferentation pain). These findings were partially confirmed by Strickland et al. (2011) who found an axotomy-induced upregulation of miR-21. Furthermore, Sakai & Suzuki (2013) could establish the role of miR-21 by pain attenuation through intrathecal administration of a direct inhibitor. An *in vitro* approach was used by Bastian et al. to show a downregulation of miR-1 (Bastian et al., 2011).

Notably, compared to Bai et al, the *in vivo* experiments concerned with neuropathic pain observed a regulation over a much larger time course, in most cases over 14 d which is consistent with previous literature data on gene regulation.

The first comparison of miRNA regulation in different pain mechanisms has been made by Kusuda et al. who analysed the expression patterns of three miRNAs (miR-1, miR-16, miR-206) in different pain conditions in both PNS and CNS. For DRG, they observed a decrease of all miRNAs in inflammatory pain but only for miR-1 and -206 in partial nerve ligation neuropathy. Interestingly, all three miRNAs were upregulated after axotomy⁴. Finally, acute nociceptive pain increased expression of miR-1 and -16 (Kusuda et al., 2011).

1.5 Neuronal Tracing

As described above, DRG consist of different cell types that seem to interact in a complex pattern. Therefore, much energy has been dedicated to better discriminate between the different fractions. One method that as proved powerful is fluorescent labelling, e.g. of neurons. Fluorescent neuronal labelling has long been established in histology to trace the course of nerve fibres or to identify neuronal subsets. Various tracers serve different purposes. Fluoroemerald (FE) is a fluorescein-labelled 10,000 Da dextran (Choi et al., 2002). As its high molecular weight impedes the permeation of intact neuronal membranes, it can be taken up only by neurons with an impaired membrane barrier function and is therefore suitable for the labelling of primarily damaged neurons (Fritsch & Sonntag, 1991). In contrast, DiI, an amphiphilic carbocyanine with two long hydrocarbon side chains, is quickly taken up by neurons and embedded in the lipid bilayer of the cell membrane where it passively diffuses

4 These findings underline the importance to distinguish between neuropathic and deafferentation pain.

along the axon (Honig & Hume, 1986). Its properties qualify DiI as a marker for neurons, and it has been established in neuronal staining (Vidal-Sanz, 1988; Sarantopoulos, 2002). Importantly, the distance between the application site and the soma (DRG) prevents accidental selection of non-neuronal tissue: Only neurons possess such long continuous branches. Double-labelling for injured vs spared neurons has mainly been described for differentiation in histology (e.g. Fluororuby and Fluorogold; Schäfers et al., 2003).

2 Objectives

The primary aim of this thesis was the investigation of possible microRNA involvement in peripheral neuropathic pain. MicroRNAs (miRNAs) have proven crucial for post-transcriptional regulation in many contexts, especially cell growth and differentiation. However, only little was known about their role in pain.

Based on findings in inflammatory pain (Bai et al., 2007) as well as the known relevance of cell growth (neurogenesis) in neuropathic pain, I postulated that specific miRNAs in the dorsal root ganglia (DRG) are regulated in the course of neuropathic pain. To this end, the miRNA expression profile is characterized in a murine model of peripheral neuropathic pain, using the established Chronic Constriction Injury (CCI) model by Bennett & Xie (1988). To obtain first information about temporal patterns as well as systemic effects, expression patterns in neuropathic and contralateral DRG at three different time points are analysed. Subsequently, significantly regulated single miRNAs are identified. For the resulting candidates, findings are validated and further analysed including histological distribution. Thus, regulation pattern and cell-specific localization of several miRNAs are characterized and linked to existent knowledge about genes involved.

In a second step, I postulated that a cell type-specific damage-related mRNA expression analysis in DRG neurons will allow a more specific and reliable method to identify new targets and the involvement of miRNAs. As DRG are of a very heterocellular nature including neuronal, immune and glial tissue, cell-type specific regulation, e.g. of neurons, might be blurred. Moreover, it has been shown that not only damaged neurons but also adjacent intact neurons undergo expression changes: A neuron-specific technique is developed that allows comparison of primarily damaged primary sensory neurons and non-damaged adjacent neurons via staining with fluorescent tracers in flow cytometry. To obtain neuron-specific information about miRNA involvement, bioinformatic prediction of miRNA involvement was conducted based on gene expression results. I hypothesized that this approach of transcriptional profiling of neuronal subpopulation will yield new insights in the respective role of damaged and intact neurons in neuropathic pain.

3 Methods⁵

3.1 Animals

For this project, female C57/BL6 mice of 6-8 weeks of age were used (Charles River, Wilmington, MA, USA). Mice were housed in sawdust cages (4-5 mice per cage, water and food provided *ad libitum*) and exposed to a circadian rhythm (light for 12h, from 6 am to 6 pm). Animal experiments were approved by EMBL Monterotondo animal committee and comply with Italian legislation (Art. 9, 27. Jan 1992, no 116) under licence from the Italian Ministry of Health.

3.2 Tissue

3.2.1 Surgery

Mice were anesthetized with an intraperitoneal injection of 1.5 ml/g 2.5% Avertin® (Tribromoethanol, Sigma Aldrich, St Louis, MO, USA) in PBS. Chronic constriction injury (CCI) was performed as follows: After fur removal in the surgery area (left proximal dorsal thigh) and skin incision (ca. 3mm), the left biceps femoris muscle was bluntly dissected at about mid-thigh level and the sciatic nerve exposed. Three friction-knotted loose ligations were tied around the sciatic nerve using 7-0 silk threads. Nerve and muscle were placed back *in situ* and the wound was closed with a 9 mm metal clip (cf. Bennett & Xie, 1988).

3.2.2 Neuronal Staining

For tracer application, surgery was performed as above. Immediately following the ligation, 2 µl of Fluoroemerald (FE, 5% in 0.9% saline) were injected epineurally into the exposed nerve proximal to the ligation site using a Hamilton syringe and a 32 G needle. Great care was taken not to penetrate deeper layers of the nerve. After closure of the wound, 4 µl DiI (1,1-dioctadecyl-3,3,3,3-tetramethylindocarbocyanine perchlorate, 10 mg/ml in DMSO, Invitrogen, Carlsbad, CA, USA) were injected subcutaneously into the plantar surface of both hind paws using a 28 G needle. The site of injection was manually pressed for one minute to facilitate puncture closure and

⁵ If not specified otherwise, all solutions and buffers used were manufactured at EMBL Monterotondo following standard protocol.

avoid dye leakage (**Fig. 4**).

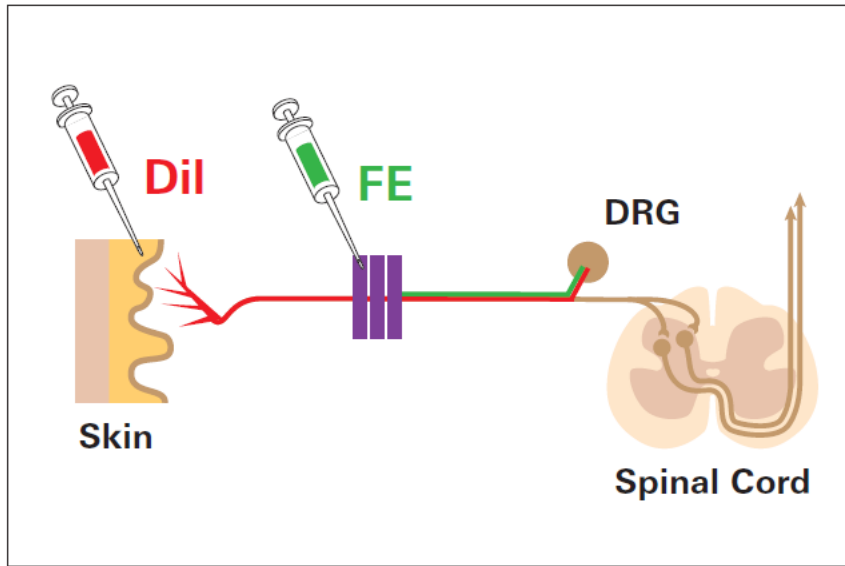


Figure 4: Principle of fluorescent tracer injection. FE (green) is injected just proximal to the site of injury (purple ligatures); it is taken up by damaged neurons and transported to the DRG. DiI (red) is injected into the hindpaw just after surgical procedure. It permeates the axonal membrane and diffuses along the axon. Membrane disruption, however, impedes further diffusion towards the DRG.

3.2.3 Tissue Collection

After a specific time-point (6 h, 1 d, 7 d respectively), mice were sacrificed by cervical dislocation. The spinal column, including surrounding tissue, was excised, followed by careful removal of vertebral bodies and the spinal cord. The proximal parts of the sciatic nerve were exposed and traced back to the respective spinal nerves. The corresponding DRG (L3-5) were excised and detached from axons and surrounding tissue before stored at -80 °C. Throughout the entire procedure, great care was taken to provide an RNase-free workplace (e.g. RNase ZAP®, Invitrogen, Carlsbad, CA, USA).

3.2.4 RNA Extraction

Tissue homogenization and RNA extraction followed standard Trizol® protocol (Invitrogen, Carlsbad, CA, USA): DRG were pooled (from 6- 10 mice per condition and run), homogenized with 1 ml Trizol reagent for 30 s and stored on ice for 10 min. After

centrifugation (12,000g at +4 °C, 10 min), supernatant was pipetted off and mixed well with 200 µl chloroform. After 3 min at room temperature (RT) the samples were again centrifuged. The resulting aqueous phase was pipetted off and washed with 100% isopropanol and 75% ethanol in RNase-free water. RNA quantity and quality were assessed by Nanodrop 8000 (Nanodrop Technologies, Wilmington, DE, USA) and Agilent 2100 Bioanalyzer (Agilent Technologies, Santa Clara, CA, USA), respectively.

3.3 Assessment of Surgical Effect

The effect of CCI in terms of neuronal damage was tested by quantitative real-time PCR, assessing the level of galanin mRNA against a reference gene. Galanin, a 30 amino acid polypeptide, has been shown to be up-regulated in DRG neurons after neuropathic pain compared to other types of pain or to naïve tissue (Ma & Bisby, 1997; Villar et al., 1989) and has hence served as a marker gene. Ubiquitin served as reference gene (Sigma-Aldrich, St Louis, MO, USA).

<i>Primers</i>	<i>Sequences</i>
Galanin	left: CTC TAG TCC TCC TGC GGT TG right: CTG GAA CCC TCC CTA CCT TC
Ubiquitin	left: TGG CTA TTA ATT ATT CGG TCT GCA T right: GCA AGT GGC TAG AGT GCA GAG TAA

After extraction as described above, RNA of ipsilateral, contralateral and naïve tissue was reverse transcribed using the *Invitrogen* SuperScript™ kit following manufacturer's protocol.

PCR master mix was prepared using 5 µl *Roche* Sybr®Green, 1 µl of 5 µM Primer Mix, and cDNA mix corresponding to 50 ng cDNA and filled up with ddH₂O to a total volume of 10 µl/replicate. For each condition, PCR was performed in triplicates. qPCR was carried out with *Roche* LightCycler® 480 (Roche, Basel, Switzerland) using the following parameters. 40 cycles were performed.

	<i>Temperature (°C)</i>	<i>Time (min)</i>
<i>Pre-Incubation</i>	95	10:00
<i>Denaturation</i>	95	00:10
<i>Annealing</i>	58	00:15
<i>Elongation</i>	72	00:10
<i>Melting Curve</i>	95	00:05
	65	01:00
	97	Cont.
<i>Cooling</i>	40	00:10

Fluorescence was measured after each cycle and cycle threshold (Ct) values calculated for each replicate. Based on respective Ct values, galanin expression level (EL) relative to ubiquitin was calculated using the following formula: $EL (Gal) = 2^{-\Delta Ct} = 2^{-(Ct(Gal) - Ct(Ubi))}$. Moreover, behaviour was observed on a daily basis. Formal algometric tests were not conducted.

3.4 MicroRNA Assay

MiRNA expression was analysed using a bead set technique (Luminex[®], Luminex Corp., Austin, TX, USA) based on solution hybridization: oligos specific to one miRNA are bound to a polystyrene bead. Per run and condition, RNA of 12 mice was pooled. 4 runs were conducted. Total RNA extracted (5 µg/sample) was spiked with three synthetic pre-labelling control RNAs (3 fmol/sample) to control for target preparation efficiency. After running a 15% polyacrylamide gel (SequaGel[®], National Diagnostics, Atlanta, GA, USA), the gel pieces corresponding to a size of 18-26 nt were cut out and eluted overnight in 0.3 M NaCl. MiRNA was ligated to 3' and 5' linkers using T4 RNA ligase, each ligation followed by gel purification. The bi-ligated products were reverse-transcribed and amplified by PCR using Biotin-labelled primers. Amplification was performed using the following parameters: 95 °C for 30 s, 50 °C for 30 s and 72 °C for 40 s (18 cycles). PCR products were precipitated and re-dissolved in TE buffer containing biotinylated post-labelling controls (100 fmol/µl).

Labelled samples were hybridized to color-coded polystyrene beads. Five distinct bead sets were used, each allowing the detecting of ~90 different miRNAs (from D. O'Carroll, EMBL Monterotondo; for further information see Blenkiron et al., 2007). Replicates were added across bead sets to guarantee comparability. Water-only blanks and bead blanks served for background noise control. Hybridization was carried out at

50 °C overnight (33 µl of bead pool and 15 µl of labelled sample per well).

<i>Oligo</i>	<i>Sequence</i>
PreControl III	pCAG UCA GUC AGU CAG UCA GUC AG
PreControl IV	pGAC CUC CAU GUA AAC GUA CAA
PreControl V	pUUG CAG AUA ACU GGU ACA AG
3' linker	pUUU aac cgc gaa ttc cag t
5' linker	acg gaa ttc ctc act AAA
Reverse transcription primer	TAC TGG AAT TCG CGG TTA
Amplification primers	5' Biotin-CAA CGG AAT TCC TCA CAT AA 3' TAC TGG AAT TCG CGG TTA

Unbound samples were removed by filtering and washing with 1x TE and 1x TMAC buffer. After re-suspension in 1x TMAC buffer, reporter protein SAPE (Streptavidin Phycoerythrin, 1:100 dilution) was added and activated by incubation at 50 °C for 10 min. Samples were transferred to a 96-well plate and processed in a Luminex 100® instrument: For each miRNA, mean fluorescence was measured.

Mean fluorescence data obtained from Luminex were processed as follows:

MiRNAs that displayed values lower than three times the background noise in all samples were removed. The remaining values were normalized based on the mean value of the pre-control samples of the respective bead set. For replicate samples, mean value and standard deviation were calculated to control for stability across bead sets. All normalized values were log₂-transformed, thus allowing a better comparison between samples. Furthermore, precontrol-normalized values were again normalized based on the naïve tissue value for each miRNA.

3.5 qRT-PCR

For selected miRNAs (mir-124, mir-137, mir-183, miR-27b and miR-505), qRT-PCR (TaqMan[®], ABI, Foster City, CA, USA) was conducted in neuropathic DRG RNA ipsi- and contralaterally at 7 d post-CCI and in naïve DRG RNA. Small nuclear RNA U6 served as a reference gene. All primers were ordered as predesigned by the manufacturer. For reverse transcription and PCR, ABI TaqMan[®] MicroRNA Reverse Transcription Kit and TaqMan[®] MicroRNA Assays were used following the

manufacturer's miRNA standard protocol⁶.

The qRT-PCR was conducted with *Applied Biosystems 7500Real-Time®* PCR System.

<i>Primer</i>	<i>Manufacturer's ID</i>
mmu-miR-124a, Rev. Transcription	RT001182
mmu-miR-124a, PCR	TM001182
mmu-miR-137, Rev. Transcription	RT001129
mmu-miR-137, PCR	TM001129
mmu-miR-183, Rev. Transcription	RT002269
mmu-miR-183, PCR	TM002269
mmu-miR-27b, Rev. Transcription	RT000409
mmu-miR-27b, PCR	TM000409
mmu-miR-505, Rev. Transcription	RT001655
mmu-miR-505, PCR	TM001655
U6 rRNA, Rev. Transcription	RT001973
U6 rRNA, PCR	TM001973

Per miRNA, two or three runs were performed, each consisting of three replicates per miRNA. Per run, DRG of ca. 6-10 mice were pooled. Ct values were calculated for each replicate. Analysis of the melting curve ensured the quality of the PCR products (i.e. no abundance of primer dimers). Expression between conditions were compared calculating $2^{-\Delta\Delta Ct} = 2^{-(\Delta Ct(\text{Condition}) - \Delta Ct(\text{Naive}))}$ for each condition, with $\Delta Ct = Ct(\text{miRNA}) - Ct(\text{U6})$.

3.6 Histology

3.6.1 In situ Hybridization

Anaesthetized mice (naïve and 7 d post-CCI) were perfused transcardially with 50 ml 4% PFA/PBS. DRG L3-L5 were dissected, fixed in 4% PFA/PBS for 2-4 h and stored in 20% sucrose/PBS at 4 °C overnight. DRG were washed in methyl butane, embedded in OCT compound and kept at -80 °C. The embedded tissue was cut in 12 µm slices and transferred onto charged object slides where the slices were allowed to dry at room temperature (RT) for 30-60 min. Slides were fixed in 4% PFA/PBS (15 min, RT) and

⁶ ABI, http://www3.appliedbiosystems.com/cms/groups/mcb_support/documents/generaldocuments/cms_042167.pdf, retrieved last Aug 18, 2013

washed in PBS (2 x 5 min), then treated with Proteinase K (10 µg/ml) (8 min, 37 °) before washed in 0.2 % Glycine in PBS (5 min) and re-fixed in 4 % PFA/PBS (15 min, RT). For acetylation, slides were treated in 0.1 M TEA, pH 8.0 (5 min), then in TEA/0.25% acetic anhydride solution (10 min). DIG-3'-labeled LNA (locked nucleic acids) probes were used (Exiqon, Copenhagen, Denmark) in a 1:1000 dilution in hybridization buffer (50% formamide, 5x SSC, 5x Denhardt's solution, 500 µg/ml salmon sperm DNA, 250 µg/ml tRNA). 100 µl of the diluted probe were applied to each slide, the slide then covered with glass cover slips.

<i>Sample</i>	<i>Sequence</i>	<i>Product No.</i>
mmu-miR-137	CTACGCGTATTCTTAAGCAATAA	38510-05
mmu-miR-183	AGTGAATTCTACCAGTGCCATA	38490-05

Hybridization was conducted in a humidified box (with 50% formamide/5x SSC) at 45°C overnight. Post-hybridization washes were performed as follows: 2x15 min in 5x SSC (RT), 30 min in 50% formamide/2x SSC (39°C), 15 min in 2x SSC, 2x15 min in PBS, 15 min in 3% H₂O₂ in PBS, 10 min in TN (Tris-Cl + NaCl) buffer (all RT). After incubation in 500 µl of 1% blocking solution for 30 min (RT, humidified box), 300 µl AntiDIG peroxidase in blocking solution (1:100) were applied to each slide for 30 min (RT). Slides were then washed 3 x 5 min in TN + 0.05% Tween (0.05% TNT). 100 µl of fluorophore in amplification solution (1:50) were applied, the slides covered with parafilm and left at RT for 7 min. Procedure was finished by washing for 3 x 5 min in 0.05% TNT and rinsing with ddH₂O.

3.6.2 Immunohistochemistry

Co-staining was conducted with fluorescent Isolectin B4 (IB4, for non-peptidergic C-fibres) and antibodies against neurofilament 200 (NF 200, for big myelinated neurons, both BioLab, Lawrenceville, GA, USA). *IB4*: slides were washed in IB4 solution and incubated in 10 µg/ml Lectina from *Bandeiraea simplicifolia*-FITC in IB4 solution (RT). *Anti-NF200*: Slides were left in 7% normal goat serum in 0.05% TNT for 30 min, followed by incubation in anti-NF200 antibody (1:4000, in 7% normal goat serum in 0.05% TNT) for 30 min at RT, then overnight at 4°C. After several washes in 0.05% TNT, slides were incubated at RT for 45 min in goat anti-mouse antibody (1:1000, in

7% normal goat serum in 0.05% TNT).

For both stainings, slides were embedded in Mowiol[®] (polyvinyl alcohol, Sigma-Aldrich) after thorough washing in 0.05 % TNT and rinsing with ddH₂O.

All pictures were taken using a Leica TCS SP5 confocal microscope (Leica, Wetzlar, Germany).

3.7 Neuron-Specific RNA Analysis

With two neuronal tracers applied ipsilaterally, four tracer combinations were possible for cell staining (cf. **table 2** for interpretation). After DRG harvest, cells were purified and sorted for both tracers. From ipsilateral neurons, two populations were sorted: FE⁻/DiI⁺ cells that were assumed to be not primarily damaged by CCI, and FE⁺/DiI⁺ cells, regarded as primarily damaged by CCI. In the following, we will refer to all ipsilateral FE⁺ cells as damaged and to ipsilateral DiI⁺/FE⁻ cells as adjacent spared. Double negative cells were not included in further analysis.

<i>FE staining</i>	<i>DiI staining</i>	<i>Interpretation</i>
+	+	Sensory neuron (hindpaw afferent), partially damaged
+	-	Sensory neuron, damaged
-	+	Sensory neuron (hindpaw afferent), not damaged
-	-	Any but the above

Table 2: Tracer combinations and their interpretation.

3.7.1 Cell Isolation and FACS

After animal sacrifice and DRG isolation as described above, DRG were sampled in D-PBS on ice and centrifuged for 1 min at 1200g (room temperature). They were then incubated in 1 mg/ml collagenase IV in DMEM and 0.05% trypsin in EDTA for 25 and 22 min, respectively, at 37 °C. Resuspended in DRG medium (10% horse serum heat-inactivated, 100 µg penicillin, 100 µg/ml streptomycin, 0.8% glucose in DMEM), cells were triturated by carefully pipetting them through 1 ml and 200 µl pipette tips and then passed through a 0.2 micron filter.

Filtered cells were resuspended in DRG medium and stored on ice. Just before cell sorting, 2 µl of Sytox®Blue (Invitrogen), a DNA-binding agent, were added to control for cell damage.

FE has a peak excitation at 495 nm and peak emission at 524 nm, whilst for DiI, peak excitation is at 551 nm and peak emission at 565 nm. Two-colour analysis was therefore carried out with blue argon excitation at 488 nm; detection channels were FITC (fluorescein isothiocyanate, peak emission at 525 nm) for FE, and PE (phycoerythrin, peak emission at 578 nm) to identify DiI.

3.7.2 RNA Extraction and Assay

RNA was extracted from sorted cells using Trizol® (see above). Isolated RNA was stored at -80°C and shipped to EMBL Heidelberg for Affymetrix Gene Expression analysis (assay: *Affymetrix Gene Expression Mouse 430_2*; conducted by Sabine Schmidt, EMBL Heidelberg).

3.8 Bioinformatics

Affymetrix Gene Expression results on mRNA were used for further bioinformatical analysis for a possible role of miRNAs. Two different web-based tools were used to minimize program-specific bias.

3.8.1 *SylArray*

SylArray (<http://www.ebi.ac.uk/enright-srv/sylarray/>, developed by Enright group, EBI Hinxton⁷) analyses over- or underrepresented miRNA-specific wordings in 3'UTRs of a gene list sorted by regulation. P-values for enrichment or depletion of each wording along the gene list are calculated in a hypergeometric approach (van Dongen et al., 2008; Bartonicek & Enright, 2010). Results are visualized for each miRNA in a chart representing enrichment or depletion along the gene list: Steep peaks suggest significant correlation to a specific gene in the gene list.

Based on Affymetrix expression data, sorted gene lists were submitted to compare a) damaged with contralateral neurons and b) damaged with adjacent spared neurons. For specificity reasons, only heptameric wordings were analysed and redundant sequences

⁷ Retrieved last Aug 18, 2013

excluded (“purging”). The general pattern was evaluated, the most significant miRNAs analysed, and the curves of candidates miR-124, -137, -183, -27b, and -505 considered. For expert evaluation of the emerging pattern, results were sent to the developers (Anton Enright, EBI Hinxton).

3.8.2 *MirAct*

MirAct (<http://sysbio.ustc.edu.cn/software/mirAct>, developed by Wu group, Shanghai) uses a different approach: Initially, single miRNA activity is assessed by comparing regulation of presumed targets with non-targets for each sample (targets are extracted from online databases like *TargetScan* or *MiRanda*, to be selected by the user), resulting in a “sample score”. In a second step, different classes of samples, i.e. conditions, are compared and a non-parametric analysis of variance performed (for details, cf. Liang et al., 2011a). Significance is calculated using the established p-value and the more recent q-value, a measure of false discovery rate. Depending on number and size of samples, several calculation parameters can be adjusted. All three classes of neurons were compared to each other in a single run. The following settings were used: Target prediction using *TargetScan 5.0*, data transformation by ranking within sample; miRNA activity determination based on sample scores. All other settings were set at default. Cluster analysis was performed based on the significance of activity alteration across classes using the q-value. As with *SylArray*, the general pattern was evaluated, the most significant miRNAs analysed, and data for miR-124, -137, -183, -27b, and -505 considered.

3.8.3 *myMIR*

To assess potential targets of miR-137 and 183, *myMIR*, a recently developed database, was used. By integrating the results of various established databases with different algorithms (*TargetScan*, *MiRanda*, *PITA*, *RNAhybrid* and *MicroT*), a resulting score is calculated on which target prediction is based. (<http://www.itb.cnr.it/micro/>, retrieved last Aug 18, 2013. For details, see Corrada et al., 2011).

3.9 Data Processing

3.9.1 Data Calculation

Data extrapolation was performed using *Microsoft Excel 2000* for Windows and *Sigmaplot 10* software.

3.9.2 Data Analysis

For qPCR experiments, significance was tested using Student's t-test (*Sigmaplot 10*). Cluster analysis for miRNA assay (*Luminex*) was executed with *Systat 13* software. For gene expression analysis, statistical analysis was performed with *GeneSpring GX* software. Data were normalized using RMA algorithm and transformed to the median of all values. Entities within the 20th -100th percentile were included in further analysis. To test significance, One-way ANOVA for unequal variance was performed, followed by Tukey HSD test. Statistical significance was determined as $p < .05$.

4 Results

4.1 CCI Produces a Neuropathy-Specific Response

To validate the effectiveness of the CCI procedure, galanin expression was quantified in RNA from CCI vs. control DRG using qRT-PCR. Although algiesiometric tests were not conducted in this experimental protocols, the CCI procedure as conducted in our working group consistently leads to a neuropathic phenotype after seven days, i.e. significant thermal and mechanical allodynia (Caspani et al., 2009). Furthermore, galanin upregulation has been shown to develop concurrent to the neuropathic phenotype (not published, personal communication PA Heppenstall). In ipsilateral DRG, results showed a steep upregulation in galanin expression over the course of 7 d (4.8-fold after 1 d, 24.3-fold after 7 d, compared to naïve control, both $p < 0.001$, $n = 3$ per group). Contralateral expression remained fairly constant (<twofold up- or downregulation, $p > 0.05$) (**Fig. 5**). Amplification of reference gene ubiquitin was reliable in all runs (standard deviation 4.1 % of mean Ct value).

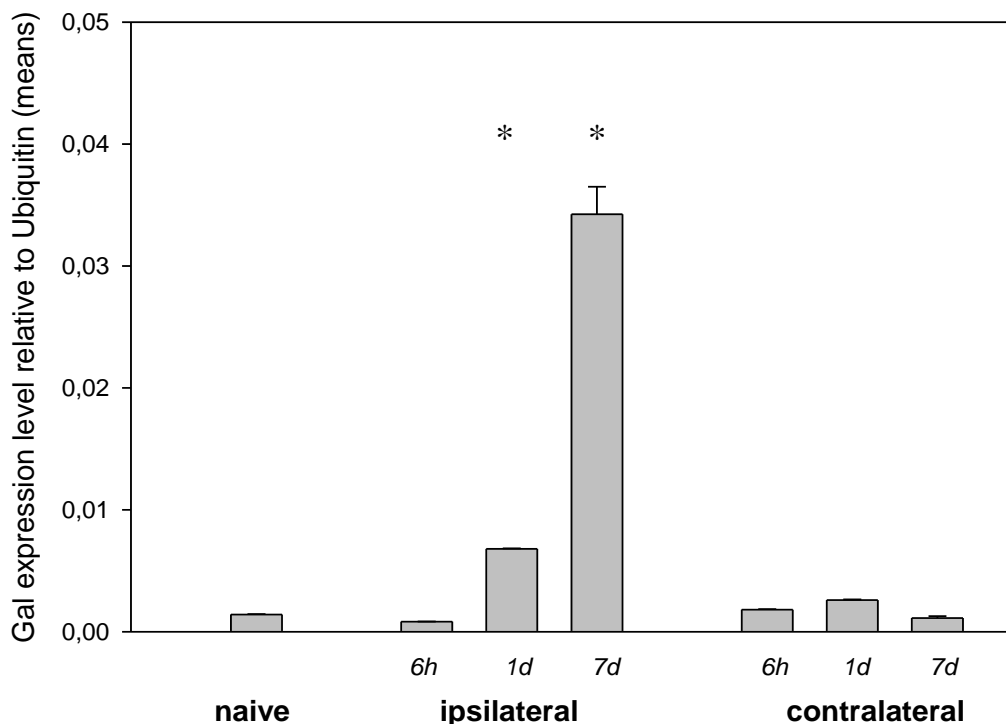


Figure 5: Galanin expression in ipsi- and contralateral DRG after 6 h, 1 d, and 7 d, compared to naïve controls. The y-axis indicates the expression relative to ubiquitin using the ΔC_t calculation model. Error bars indicate standard deviation. Asterisk denotes $p < 0.001$ compared to naïve DRG. $n = 3$ per group, 12 mice per run).

4.2 MicroRNAs are Regulated in CCI

4.2.1 Increase in microRNA Regulation over Time

To assess development of miRNA regulation, expression was assessed at three different time points: 6 h post-surgery, after a latency of 1 d, and after 7 d. Four runs of Luminex assay were performed, one of which was excluded from further analysis due to low expression values (less than 10% of miRNAs showed signals considerably (>3fold) above background signalling). Per run and condition, RNA from 12 animals was pooled. As for the three runs included in further analysis, cluster analysis of the expression profile showed the 7 d samples as most divergent from control samples, with the ipsilateral expression pattern being more distinct than the contralateral (**Fig. 6**). Hence, further experiments focus exclusively on expression after 7 d.

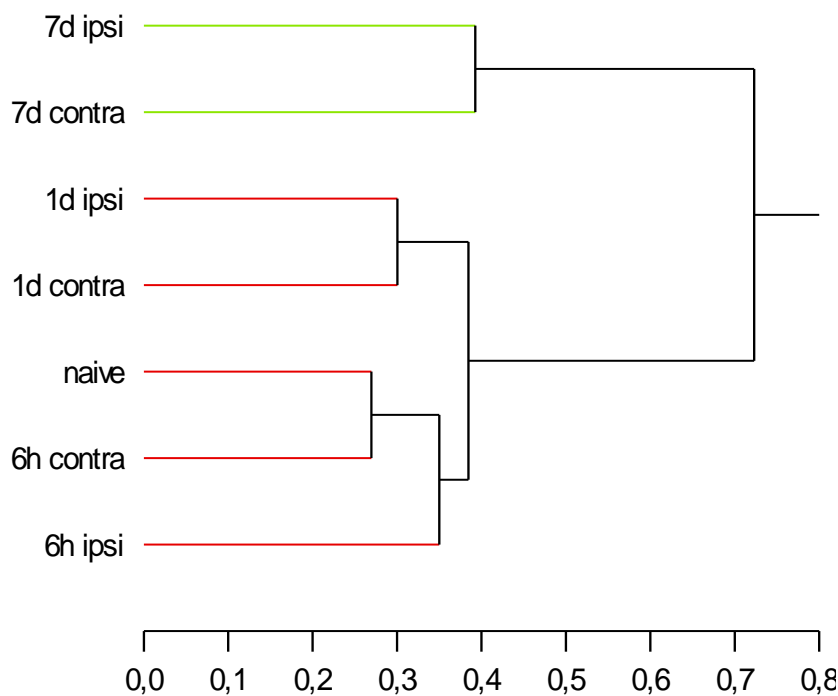


Figure 6: Condition-based cluster analysis of miRNA assay data. X-axis denotes distance. The graph shows an increasing distance over time with a clear distinction bilaterally after 7 d (distance metric Euclidean distance; average linking method. n=3, 12 mice per run)

4.2.2 Predominantly Downregulation of microRNAs

The number of regulated miRNAs in neuropathic neurons varied considerably between runs. Only a few miRNAs showed a consistent and distinctive up- or downregulation (>twofold) against naïve DRG tissue. Few miRNAs were upregulated compared to the number of downregulated genes. Table 3 gives an overview of relevant miRNAs; included are all miRNAs downregulated in 7 d ipsilateral compared to naïve DRG in at least one run. In table 4, miRNAs that either show a >twofold upregulation in 7 d ipsilateral against naïve DRG or an upregulation <twofold plus a discrepancy between ipsi- and contralateral tissue are included.

	<u>RUN 1</u>			<u>RUN 2</u>			<u>RUN 3</u>	
	7 d ipsi	7 d contra		7 d ipsi	7 d contra		7 d ipsi	7 d contra
			let-7a	0.43	0.45	let-7a	0.48	0.50
			let-7c	0.40	0.47	let-7c	0.48	0.50
let-7f	0.48	0.60	let-7f	0.47	0.48			
			miR-1	0.46	0.44	miR-1	0.50	0.45
						miR-103	0.45	0.60
						miR-107	0.44	0.60
miR-124	0.33	0.59	miR-124	0.28	0.40	miR-124	0.39	0.53
			miR-126-5p	0.46	0.57	miR-126-5p	0.50	0.49
			miR-128a	0.47	0.64	miR-128a	0.43	0.59
			miR-128b	0.33	0.49	miR-128b	0.35	0.57
						miR-130a	0.49	0.67
			miR-136	0.41	0.51	miR-136	0.43	0.54
miR-137	0.36	0.58	miR-137	0.24	0.30	miR-137	0.32	0.34
miR-138	0.41	0.50	miR-138	0.41	0.60	miR-138	0.50	0.63
miR-16	0.38	0.51						
			miR-181b	0.50	0.72			
						miR-182	0.50	0.51
miR-183	0.47	0.73	miR-183	0.42	0.53	miR-183	0.50	0.54
						miR-193	0.30	0.37
miR-24	0.36	0.51						
			miR-26a	0.49	0.58			
			miR-26b	0.43	0.50	miR-26b	0.45	0.46
						miR-29a	0.50	0.55
miR-29b	0.42	0.54	miR-29b	0.28	0.44	miR-29b	0.34	0.48
			miR-29c	0.37	0.48	miR-29c	0.40	0.50
			miR-30d	0.40	0.52	miR-30d	0.43	0.54
						miR-320	0.34	0.43
			miR-33	0.43	0.55	miR-33	0.32	0.38
miR-338-3p	0.49	0.72						
						miR-34a	0.45	0.61
			miR-382	0.49	0.55	miR-382	0.38	0.44
			miR-674	0.46	0.75	miR-674	0.46	0.63

miR-700	0.49	0.74			
miR-7b	0.35	0.51	miR-7b	0.38	0.49
miR-7d	0.42	0.57	miR-7d	0.48	0.53
			miR-96	0.48	0.57

Table 3: miRNA downregulation 7 days after CCI. Shown are expression levels (ipsi- and contralaterally) relative to naïve DRG; included are all miRNAs with an ipsilateral downregulation by $\geq 50\%$ in at least one Luminex® run. Highlighted are miRNAs that exhibit consistent downregulation in all three runs.

<u>RUN 1</u>		<u>RUN 2</u>		<u>RUN 3</u>		
7 d ipsi	7 d contra	7 d ipsi	7 d contra	7 d ipsi	7 d contra	
(none)				miR-215	2.05	1.12
	miR-27b	1.46	0.65	miR-27b	1.72	0.70
	miR-505	1.37	0.87	miR-505	1.85	1.20

Table 4: miRNA upregulation 7 days after CCI. Shown are expression levels (ipsi- and contralaterally) relative to naïve DRG; included are all miRNAs with an ipsilateral upregulation by $\geq 50\%$ in at least one Luminex® run. No miRNA exhibits consistent upregulation in all three runs.

From the assay runs, five miRNAs were chosen for further validation and analysis: miR-124, miR-137 and miR-183 had been downregulated in all three runs. MiR-27b and miR-505 were selected for they showed an unusual expression pattern in two runs, i.e. a considerable (though < 2 -fold) differential regulation ipsilaterally as well as a high discrepancy between ipsi- and contralateral DRG. Two miRNAs, miR-138 and miR-29b, were not included in qPCR despite interesting initial results. Restrictions were mandatory due to resource limitations; exclusion criteria were little suggestive data in literature compared to the other three downregulated miRNAs (miR-124, miR-137, miR-183).

4.3 Validation of Regulation Patterns for Selected microRNAs

Two to three runs of qPCR analysis of miRNA candidate expression were performed, for each run and condition, RNA from 12 mice was pooled. While quality control with housekeeping gene snRNA U6 remained robust (mean standard deviation 3.4 % of mean Ct), results of repetitive runs were highly divergent. In the following, the terms “run 1”, “run 2” etc. are referring to each miRNA individually, i.e. “run 1” for miR-27b does not refer to the same sample as “run 1” for miR-505.

4.3.1 miR-183

Two qPCR runs showed a significant down-regulation ipsilaterally by 39 % after 7 d (mean=.61, standard deviation ± 0.09 , $p < .05$) and by 29 % contralaterally (mean=.71, standard deviation $\pm .27$, n.s.) (**Fig. 7a**).

4.3.2 miR-137

Three qPCR runs were performed on miR-137. Overall comparison showed a down-regulation of miR-137 by 32% ipsilaterally (mean=.68, standard deviation $\pm .44$, n.s.) and 3% contralaterally (mean=.97, standard deviation $\pm .14$, n.s., **Fig. 7b**). However, none of these results were significant due to high divergence between runs: Concentration in 7 d ipsilateral DRG RNA compared to naïve tissue RNA varied from 39 to 118%. Also, the relation of 7 d ipsi- to contralateral RNA differed between 40 and 106%.

4.3.3 miR-124

Two qPCR runs on miR-124 yielded contradictory results regarding its regulation after 7 d, best seen in a 3D plot comparing both results: Concentration in 7 d ipsilateral DRG RNA compared to naïve tissue RNA varied from 72 to 156%. In both runs, expression had changed consensually in ipsi- and contralateral tissue (**Fig. 8a**).

4.3.4 miR-505

A similar pattern emerged for miR-505. As shown in **figure 8b**, both runs showed conflicting expression patterns. Expression in 7 d ipsilateral DRG diverged between 54 and 311% of naïve controls. Also here, 7 d ipsi- and contralateral expression showed the same trend in each run.

4.3.5 miR-27b

Also for miR-27b, two runs were performed with contradictory results (**Fig. 8c**). Concentration in 7 d ipsilateral DRG RNA compared to naïve tissue RNA varied from 21-133%. Moreover, there is no consistent pattern between 7 d ipsi- and contralateral

RNA to be found.

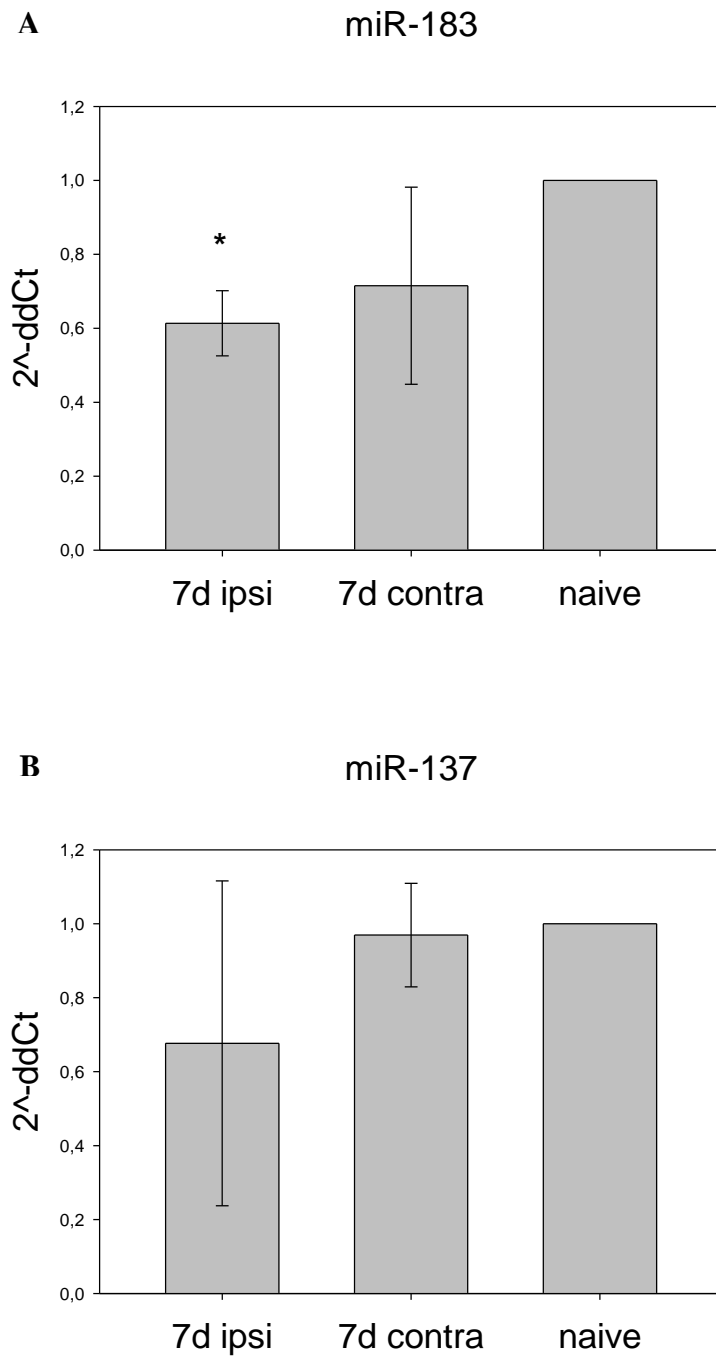


Figure 6: miRNA expression of miR-183 (A) and miR-137 (B) in ipsi- and contralateral DRG 7 d after CCI relative to naïve control. Error bars mark standard deviation, n=3. Asterix: $p \leq 0.05$ (ANOVA). Both miRNAs are downregulated. Due to high divergence in miR-137, though, differences are significant only for miR-183 (ipsilaterally).

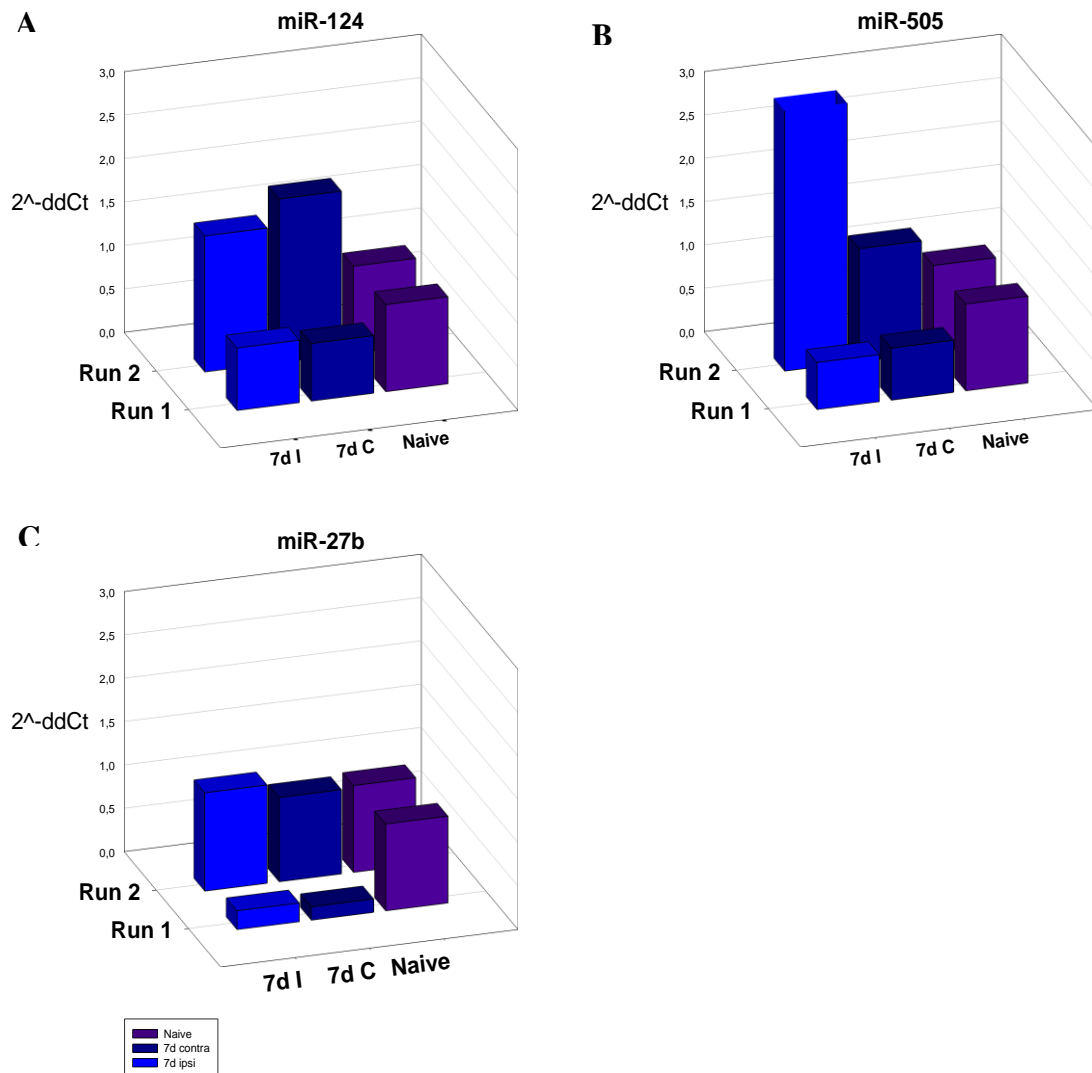


Figure 8: Expression of miR-124 (A), -505 (B) and -27b (C) in ipsi- and contralateral DRG 7 d after CCI, compared to naïve control. Both runs conducted are displayed separately to display their divergence. Data based cycle threshold values relative to U6. (7 d I: ipsilateral, 7 d C: contralateral)

4.4 *In Silico* Target Prediction for Selected microRNAs

For miR-183, 694 putative target genes were predicted; 646 for miR-137. The top 20 results of each are listed in tables 5 and 6.

<i>Gene</i>	<i>Site</i>	<i>Score</i>	<i>Pita</i>	<i>TargetScan</i>	<i>MiRanda</i>	<i>MicroT</i>
D19Wsu162e	WW protein domain 1 like	5.540	-15.93	-0.476	-24.35	.00
Bysl	bystin	5.234	-12.38	-0.519	.00	.00
Cyp2c38	Cytochrome P450 2c38	5.201	-6.21	-0.432	.00	4.00
Cdc37l1	Cell division cycle 37-like 1	5.198	-7.11	-0.410	.00	.00
Prr16	Proline-rich protein 16	5.121	-6.56	-0.461	.00	.00
Slc35a4	Solute carrier family 35, member A4	5.116	-7.79	-0.366	.00	.00
Trhr	Thyrotropin-releasing hormone receptor	5.094	-14.40	-0.435	-22.71	.00
Pak2	p21 protein (Cdc42/Rac)-activated kinase 2	5.051	-8.00	0-.365	.00	10.35
Prkd3	Protein kinase C δ3	5.014	-6.16	-0.461	.00	4.00
Sik1	Salt-inducible kinase 1	5.002	-5.47	-0.381	.00	18.92
Rhag	Rh-associated glycoprotein CD241	4.981	-7.59	-0.368	.00	.00
Zfp516	Zinc finger protein 516	4.963	-7.21	-0.339	.00	.00
Ap3s1	Adaptor-related protein complex 3, sigma 1 subunit	4.960	-5.08	-0.502	.00	.00
Ccny	Cyclin-Y	4.954	-7.58	-0.221	.00	21.01
Mlc1	Membrane protein MLC1	4.950	-7.36	-0.413	.00	10.35
Tjp2	Tight junction protein 2	4.947	-6.45	-0.340	.00	.00
Dmrt3	Doublesex and mab-3 related transcription factor 3	4.930	-4.50	-0.510	.00	.00
Tssk1	Testis-specific serine kinase 1	4.918	7.26	-0.448	.00	.00
Dmrt2	Doublesex and mab-3 related transcription factor 2	4.913	-4.46	-0.510	.00	.00
Slc37a1	Solute carrier family 37, member 1	4.902	-9.14	-0.291	.00	.00

Table 5: Top putative target genes for miR-183, according to myMIR analysis (ranked by score)

<i>Gene</i>	<i>Site</i>	<i>Score</i>	<i>Pita</i>	<i>TargetScan</i>	<i>MiRanda</i>	<i>MicroT</i>
Tdgf1	Teratocarcinoma-derived growth factor 1	5.388	-24.5	-0.457	-32.90	8.01
Pdcd4	Programmed cell death protein 4	5.202	-14.6	-0.319	.00	.00
Sel1l	Suppressor/enhancer of Lin-12-like	5.190	-15.32	-0.370	-27.26	22.42
Foxn2	Forkhead box N2	5.121	-18.58	-0.217	-25.81	.00
Dgcr2	DiGeorge syndrome critical region gene 2	5.120	-12.21	-0.292	-20.23	9.88

Zdhc6	Zinc finger DHHC-type containing 6	5.045	-11.72	-0.228	.00	8.16
Npc2	Niemann-Pick disease, type C2	4.983	-13.28	-0.443	-20.90	15.62
Arhgap26	Rho GTPase activating protein 26	4.934	-11.51	-0.303	.00	.00
Nr3c1	Nuclear receptor subfamily 3, group C, member 1 (glucocorticoid receptor)	4.901	-10.07	-0.252	.00	12.45
Kif2a	Kinesin heavy chain member 2A	4.890	-11.31	-0.360	-20.96	14.16
Rnf138	Ring finger protein 138, E3 ubiquitin protein ligase	4.865	-11.02	-0.282	.00	.00
Tcf7l2	Transcription factor 7-like 2	4.791	-11.27	-0.210	-20.12	.00
Slc16a12	Solute carrier family 16, member 12	4.785	-8.36	-0.332	.00	1.00
Cd300e	CD300e, immune receptor expressed by myeloid cells (IREM)-2	4.780	-14.17	-0.359	-21.54	6.01
Clic5	Chloride intracellular channel protein 5	4.771	-14.95	-0.226	.00	.00
Arhgap12	Rho GTPase activating protein 12	4.769	-6.46	-0.431	.00	22.82
Cep97	Centrosomal protein of 97 kDa	4.767	-12.13	-0.450	.00	.00
Ss18	Synovial sarcoma translocation, chromosome 18	4.761	-7.34	-0.389	.00	6.01
Zfpn2	Zinc finger protein, FOG family member 2	4.745	-11.85	-0.294	-20.97	.00
Csf1r	Colony stimulating factor 1 receptor, CD115	4.732	-13.88	0.000	-24.79	.00

Table 6: Top putative target genes for miR-137, according to myMIR analysis (ranked by score)

4.5 Localization of miR-183 and miR-137 in DRG

Chromogenic *in situ* hybridization in ipsilateral and naïve DRG was performed for miR-137 and miR-183 (**Fig. 9**). Additionally, for miR-137, fluorescent *in situ* hybridization with immunohistochemistry for markers of neuronal subsets was conducted. MiR-137 appeared in both ipsilateral and naïve DRG. Consistent with chromogenic staining that suggested a preference for small neurons, co-staining showed a nearly exclusive location of miR-137 in IB-4-positive cells but no overlap with NF200-positive cells (**Fig. 10**). There was no distinct difference in absolute concentration or in intracellular distribution detectable. For miR-183, chromogenic ISH did not show quantifiable differences between ipsilateral or naïve samples. Furthermore, its expression could not

be attributed to specific cell types.

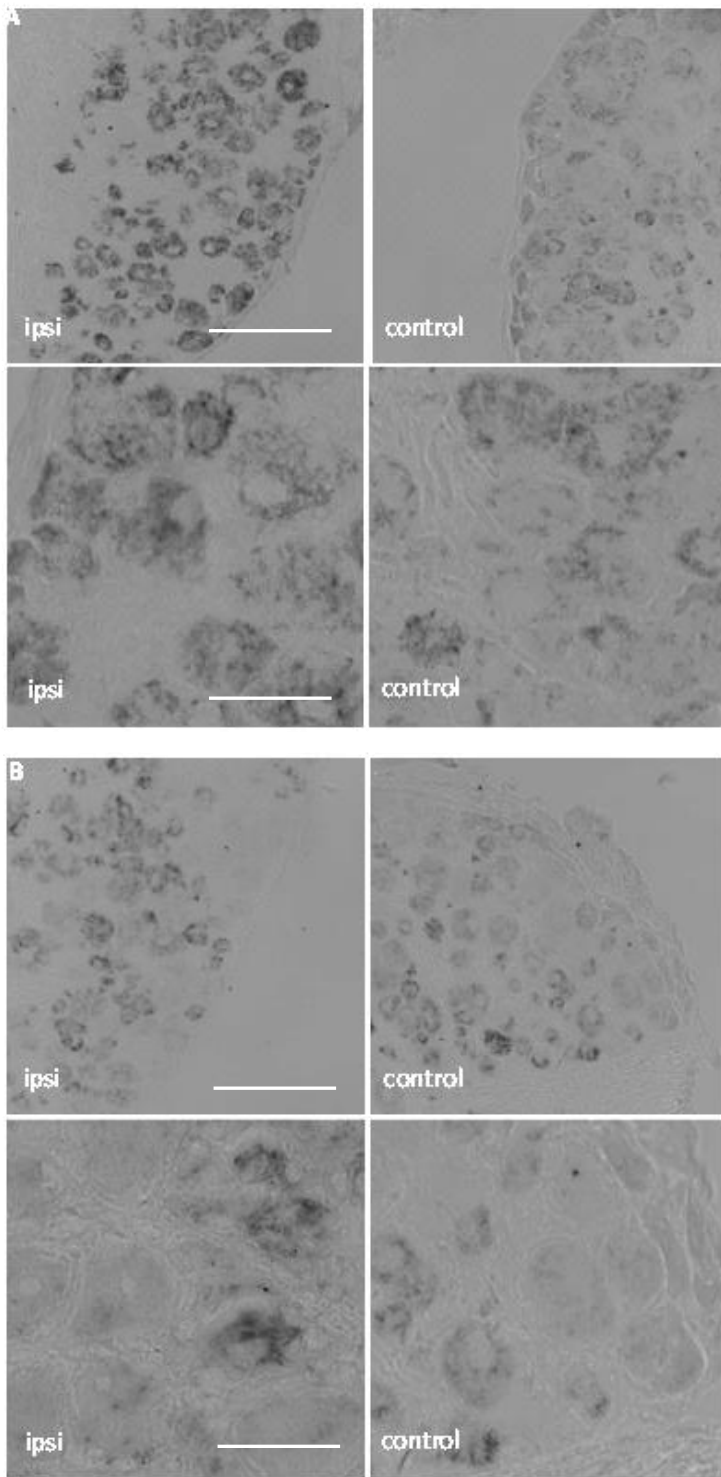


Figure 9: Chromogenic staining of miR-183 (A) and -137 (B). Above overview (scale bar=100µm), below close-up (scale bar=25µm). Each for ipsilateral and naïve control DRG. Representative examples, n=8). No staining was seen after omission of the probe.

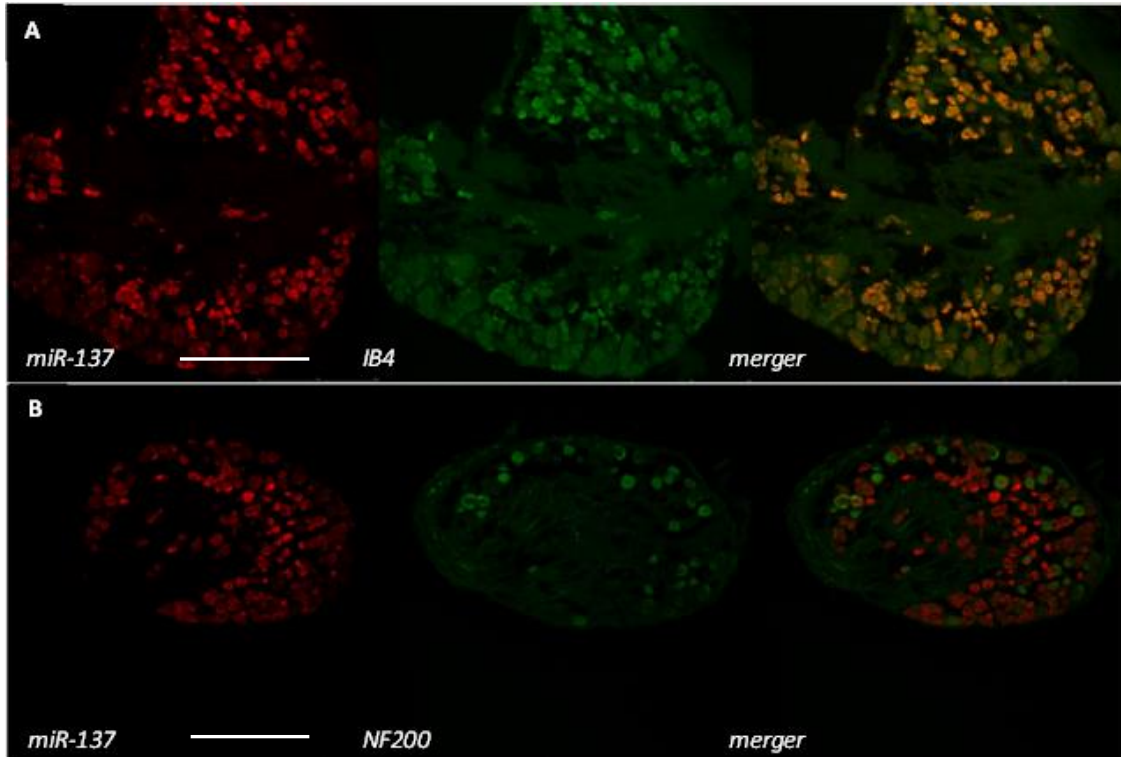


Figure 10: Fluorescent in-situ hybridization of naïve DRG for miR-137 with IB4 (A) and NF200 (B). The merged pictures show a co-localization of miR-137 and IB4, but not with NF 200 (collaboration with Daniele Hasler). Representative sample, n=8, scale bar =250 μ m). No staining was seen after omission of the probe or of primary antibodies.

4.6 Neuronal Tracing allows Distinction between Damaged and Intact Neurons

To allow for detection of cell type-specific regulation, a neuron-specific approach was developed to compare primarily damaged DRG neurons, adjacent spared neurons and contralateral DRG neurons, with the latter serving as control. Thus, blurring effects by other cell types like glia, be they differentially regulated or unaltered, could be avoided. After gating for size, granularity and viability, the remaining cells were sorted for DiI and FE (Fig 12). The sorting of marked damaged and non-damaged neurons yielded between 5790 and 12140 FE⁺ cells, between 5470 and 22553 DiI⁺/FE⁻ cells ipsilaterally and 2304 and 19644 DiI⁺ cells contralaterally in three runs (n=12 mice per run).

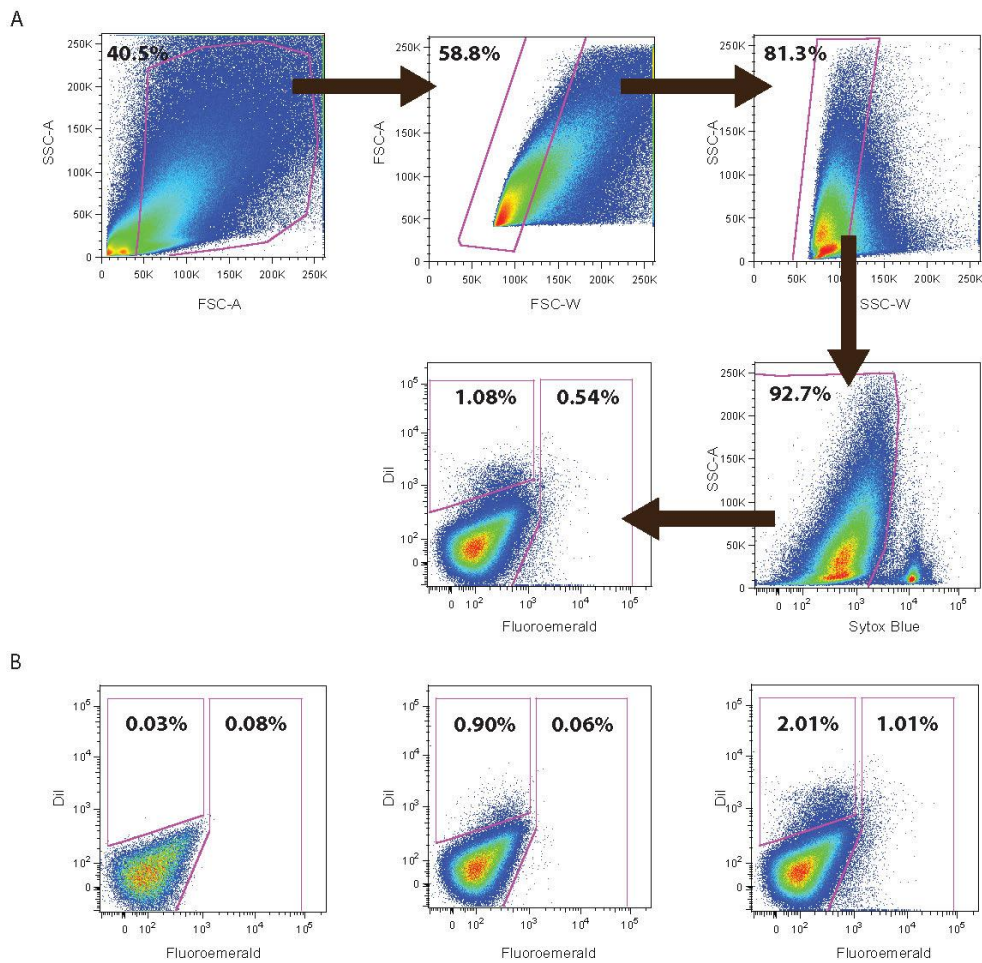


Figure 12: Representative example of flow cytometry. The sorting strategy to identify neurons positive for Fluoroemerald (FE) and DiI is shown in (A). Initially, cells were gated for size and granularity, before excluding dead cells using Sytox Blue. The remaining cells were sorted for DiI and FE. FACS plots of negative control (B left), contralateral (B middle) and ipsilateral (B right) DRG cells. DiI⁺/FE⁻ cells are considered to be intact neurons, FE⁺ cells are damaged neurons. Both populations were obtained for further analysis (n = 3, representative sample).

4.7 Distinct mRNA Expression Patterns in Damaged vs Intact DRG Neurons after CCI

From sorted cells, RNA was purified and further analysed using the *Affymetrix* Gene Expression array. mRNA expression in primarily damaged neurons was compared with adjacent non-damaged neurons of the same DRG and with neurons of contralateral corresponding DRG. Though replicates do show a certain disparity, the correlation plot

reveals a high overlap within the damaged and contralateral classes, respectively. Samples of adjacent, non-damaged neurons, however, exhibit a broader variety (Fig. 12).

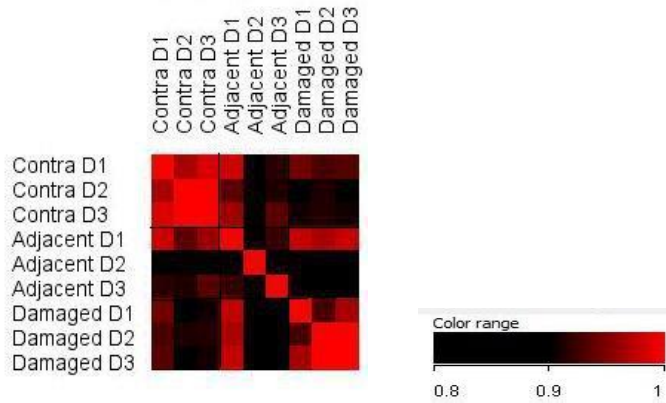


Figure 12: Microarray similarity analysis. Whilst samples of damaged and contralateral cells show a high within-group similarity, this cannot be found in adjacent non-damaged cells. (D1-3: run (‘day’) 1-3).

Principle Component Analysis (PCA) transforms several correlated variables into a small number of uncorrelated variables called *principal components* that account for a major part of the variability in the data. It confirms the previous analysis (Fig. 13).

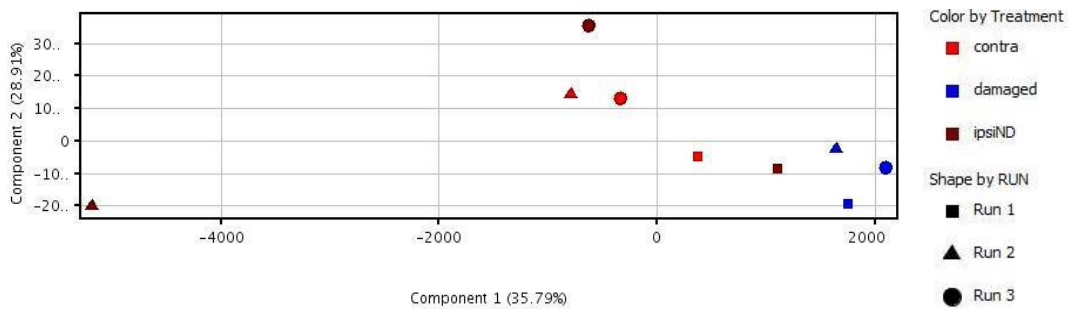


Figure 13: Principal component analysis on microarray. The two major components account for 65.7% together. A clear disparity of adjacent cells in run 2 can be observed. (IpsiND= adjacent).

4.7.1 Class Comparison of mRNA Regulation

45,101 genes were included in further analysis. In ANOVA analysis, 3,741 genes showed a significant variance between two classes ($p \leq 0.05$). Table 7 reports genes differentially expressed in class comparison. Furthermore, post-hoc analysis of

intersections shows a high overlap of the contra-vs-damaged and the adjacent-vs-damaged comparisons: 1014 genes are differentially regulated in damaged neurons compared to both contralateral and adjacent neurons. This number is considerably higher than for contralateral (377) and adjacent (332) neurons and underlines the unique expression pattern.

4.7.2 Differentially Regulated Genes after CCI

As this thesis is primarily concerned with the expression and regulation of miRNAs in neuropathic pain, the extensive results of Gene Expression Microarray will be summarised only briefly here: Top-regulated genes are listed in the following tables, followed by a more detailed description of genes known to play a role in neuropathic pain, like ion channels and neuropeptides.

	<i>Damaged</i>	<i>Adjacent</i>	<i>Contralateral</i>
<i>vs. damaged</i>	--	1930	897
<i>vs. adjacent</i>	1930	--	1498
<i>vs. contralateral</i>	897	1498	--
<i>vs. other two conditions</i>	1014	332	377

Table 7: Group differences (microarray). Number of genes expressed differentially in two treatments. Last row: Intersection of two pairs, i.e. expression differential to both other treatments (n=3, one-way ANOVA and Tukey post-hoc testing).

4.7.2.1 Damaged vs. Contralateral DRG Neurons

<i>Gene</i>	<i>Upregulation</i>	<i>Gene Information</i>	<i>p-value</i>
Crh	209.04	Corticoliberin	0.019
Sprr1a	34.48	Small proline-rich protein 1A	0.030
Inhbb	25.16	Inhibin β -B	0.007
Neto1	19.85	Neuropilin and tolloid-like 1	0.014
Serpinb1a	17.00	Serine peptidase inhibitor B 1a	0.021
Gpr151	14.08	G protein-coupled receptor 151	0.021
Shisa9	14.00	Shisa homolog 9	0.027

Speer1-ps1	12.76	Spermatogenesis assoc. glutamate-rich protein 1, pseudogene 1	0.029
Lmo7	11.81	LIM domain only 7	0.022
Cckbr	11.11	Cholecystokinin B receptor	0.014
Sdc1	10.69	Syndecan 1	0.035
Sox11	10.67	SRY-box containing gene 11	0.029
Nts	10.61	Neurotensin	0.010
Mmp16	10.60	Matrix metalloproteinase 16	0.044
Chac1	8.48	Cation transport regulator-like 1	0.026
Otop1	8.39	Otopetrin 1	0.001
P2rx3	8.19	Purinergic receptor P2X 3	0.032
Sez6l	7.94	Seizure-related 6 homolog like	0.043
Bcat1	7.44	Branched chain aminotransferase 1, cytosolic	0.041
Gal	7.19	Galanin	0.030
Fgf3	6.92	Fibroblast growth factor	0.042
Ecel1	6.70	Endothelin converting enzyme-like 1	0.035
Anxa1	5.26	Annexin A1	0.046

Table 8: Genes upregulated (>5-fold) in damaged DRG neurons compared to contralateral control (n=3).

<i>Gene</i>	<i>Downregulation</i>	<i>Gene Information</i>	<i>p-value</i>
Ripk4	27.41	Receptor-interacting serine-threonine kinase 4	0.006
Aqp4	27.11	Aquaporin 4	0.002
Bcan	24.75	Brevican	0.003
2900052N01Rik	24.41		0.004
Ptprz1	22.37	Protein tyrosine phosphatase receptor Z1	0.009
Rlbp1	22.37	Retinaldehyde binding protein 1	0.004
Plscr2	17.27	Phospholipid scramblase 2	0.004
Lect1	17.24	Leukocyte cell derived chemotaxin 1	0.020
Acsbg1	16.74	Acyl-CoA synthetase bubblegum family member 1	0.003
Hey2	16.50	Hairy/enhancer-of-split related with YRPW motif 2	0.009
Fbln5	16.49	Fibulin 5	0.007
Fbln2	16.08	Fibulin 2	0.003
Spon1	16.01	Spondin 1	0.006
Gja1	15.12	Gap-junction protein α 1	0.009

Aldoc	14.25	Aldolase C	0.005
Pcdh10	14.11	Protocadherin 10	0.000
Hes5	14.06	Hairy and enhancer of split 5	0.015
Rassf10	14.04	Ras association domain family member 10	0.014
Jam2	13.80	Junction adhesion molecule 2	0.003
Ttyh1	13.71	Tweety homolog 1	0.010
Tyrrp1	13.58	Tyrosinase-related protein 1	0.006
Elovl2	13.55	Elongation of VLC fatty acids-like 2	0.004
Mmd2	13.38	Monocyte-macrophage differentiation-associated 2	0.014
Fmo1	13.07	Flavin containing monooxygenase 1	0.004
Tmem47	12.98	Transmembrane protein 47	0.005
Cdh11	12.28	Cadherin 11	0.010
Atp1a2	12.08	ATPase, Na ⁺ /K ⁺ -transporting α 2	0.006
Megf10	11.88	Multiple EGF-like Domains 10	0.005
Cxcr7	11.57	Chemokine (CXC) receptor 7	0.005
Cybrd1	11.57	Cytochrome b reductase 1	0.010
Slc35f1	11.45	Solute carrier family 35, F1	0.007
Fam181b	11.26	family with sequence similarity 181, member B	0.011
Lgr5	11.20	Leucine rich repeat containing GPCR 5	0.010
Fhdc1	11.19	FH2 domain containing 1	0.014
Prss35	11.18	Serine protease 35	0.017
Ptgfrn	11.17	Prostaglandin F2 receptor negative regulator	0.005
Copg2as2	10.85	Coatmer protein complex, γ 2, antisense 2	0.003
Ndnf	10.80	Epidermacan	0.005
Rbp1	10.54	Retinol binding protein 1	0.017
Gpr3711	10.44	GPCR 37-like 1	0.011
Nfe2l3	10.38	Erythroid derived nuclear factor 2 like 3	0.006
Vwc2	10.37	Von-Willebrand Factor C2	0.002
Ptn	10.35	Pleiotrophin	0.004
Itih5	10.18	Inter-alpha inhibitor H5	0.021

Table 9: Genes downregulated (> 10-fold) in damaged DRG neurons compared to contralateral control (n=3).

4.7.2.2 Damaged vs. Adjacent Spared DRG Neurons

Gene regulation in damaged neurons compared to their intact neighbours shows the same trend as regulation compared to contralateral neurons, yet to a smaller degree. A list of the most up- and downregulated genes can be found in **tables 10 and 11**.

<i>Gene</i>	<i>Upregulation</i>	<i>Gene Information</i>	<i>p-value</i>
Neto1	20.86	Neuropilin and tolloid-like 1	0.014
Serpinb1a	11.72	Serine peptidase inhibitor, clade B, member 1a	0.021
Shisa9	11.61	Shisa homolog 9	0.027
Sox11	10.91	SRY-box containing gene 11	0.025
Inhbb	8.56	Inhibin beta-B	0.007
Mmp16	8.18	Matrix metalloproteinase 16	0.044
Gpr151	7.85	G protein-coupled receptor 151	0.021
Cckbr	6.18	Cholecystokinin B receptor	0.015
Lmo7	5.69	LIM domain only 7	0.020
Bcat1	5.68	Branched chain aminotransferase 1	0.041
Sez6l	5.65	Seizure-related 6 homolog like	0.043

Table 10: Genes upregulated (>5-fold) in damaged DRG neurons compared to adjacent non-damaged neurons (n=3).

<i>Gene</i>	<i>Downregulation</i>	<i>Gene Information</i>	<i>p-value</i>
Aqp4	18.22	Aquaporin 4	0.002
Bcan	15.24	Brevican	0.003
Ptprz1	14.12	Protein tyrosine phosphatase Z 1	0.010
Fbln5	12.37	Fibulin 5	0.007
2900052N01Rik	11.40		0.004
Gjar1	10.96	Gap junction protein alpha 1	0.009
Fbln2	10.03	Fibulin 2	0.003

Table 11: Genes downregulated (>10-fold) in damaged DRG neurons compared to adjacent non-damaged neurons (n=3).

Post-hoc analysis revealed 1,014 genes differentially regulated in damaged neurons compared to both contralateral and adjacent non-damaged DRG neurons. Of these, only

11 exhibited opposed regulation for damaged and adjacent neurons. The vast majority, 820, showed a regulation in damaged neurons that was larger compared to contralateral than to adjacent neurons.

4.7.2.3 Regulated Ion Channels

As ion channels have been shown to play a crucial role in sensitization and ectopic discharge in neuropathic pain, special attention was paid to their expression and regulation in the Affymetrix® array. RNA of four channels was considerably upregulated (> twofold) in damaged compared to contralateral neurons in all three runs: Purinergic receptor P2x3, an ATP-gated ion channel (Ca²⁺ affine), voltage-gated calcium channel alpha 2 delta subunit 1 (Cacnα2δ1), voltage-gated potassium channel Q2 (Kcnq2) and anoctamin 4, a calcium-activated chloride channel of the TMEM16 family. Other upregulated proteins that regulate ion flux are cation transport regulator-like 1 (Chac1) and Otopetrin (Otop1).

Down-regulated channels include various potassium channels (Kcnj10, Kcnn4, Kcnk2, Kctd1) but also transient receptor potential channel Trpm3 and Scn3b, encoding for TTX-S Na_v1.3. Further channels like Trpa1 and TTX-R Na_v1.8 and 1.9 are down-regulated in two runs.

4.7.2.4 Regulated Peptides

Of the classical signalling neuropeptides known to be involved in neuropathic pain, galanin was considerably upregulated in damaged neurons (7.19-fold compared to contralateral neurons, 3.76-fold compared to adjacent neurons). Furthermore, CGRP target chemokine ligand Ccl2 was found upregulated in damaged neurons in two runs: between 2.2- and 2.9-fold compared to contralateral neurons and between 1.5- and 3.0-fold to adjacent neurons. Substance P was not tested in the microarray, while Neuropeptide Y and CGRP were eliminated from the ANOVA due to highly divergent expression values within the conditions.

4.7.2.5 Regulation of microRNA Top Targets

Of the top 20 targets as listed by myMIR, only two targets for each miRNA are significantly regulated in the array (p<.05), although to modest extent: For miR-137

targets *Clic5* (chloride intracellular channel 5) and *Zfpn2* (zinc finger protein 2), upregulation levels are below 1.5-fold in damaged neurons. For miR-183, regulated targets include *Prkd3* (protein kinase C δ 3) and *Mlc1* (membrane protein MLC1). While the first is only little upregulated (below 1.5-fold), *Mlc1* was surprisingly downregulated by >9-fold compared to contralateral and by >7-fold compared to adjacent neurons.

4.8 *In Silico* Deduction of miRNA Involvement after CCI

Based on Affymetrix expression data, bioinformatics were applied to deduce a possible role of miRNAs.

4.8.1 *SylArray* Analysis

Compared against contralateral neurons, a significant ($p < .01$) enrichment or depletion of 7-mer-wordings at some point along the sorted gene list was identified for 42 miRNAs. The three most significantly enriched wordings corresponded with miR-706, -26a, and -377, the three most significantly depleted wordings matched miR-297b-3p, -1933-5p, and -698. Yet, the graphic visualization, did not display a distinctive pattern in any of them corresponding with a specific subset of genes (**Fig. 14**).

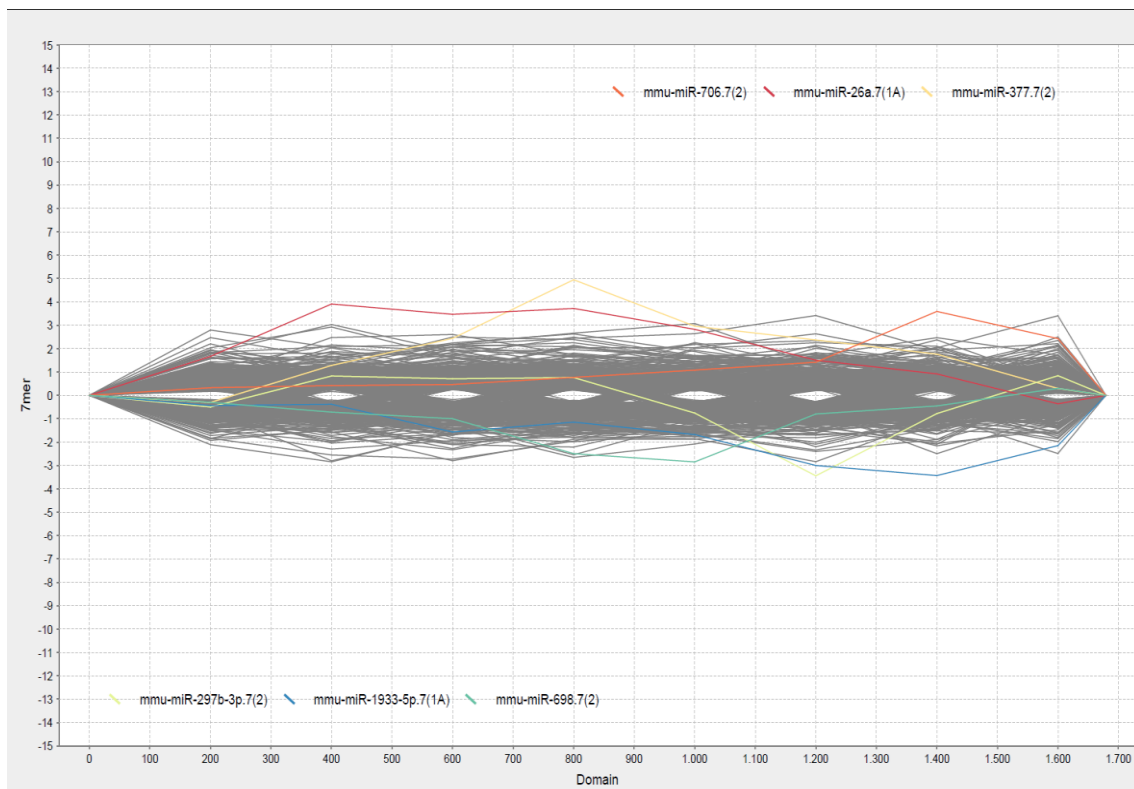


Figure 14: *SylArray* graph of wording regulation in damaged vs. contralateral DRG neurons. Genes are sorted by change in expression, in decreasing order. Y axis shows the log of enrichment/depletion p-value for 7-mer miRNA seeds in 3'UTR. Included are all miRNAs with a p-value of $p < 0.1$. Coloured lines represent the 6 most significant miRNA seeds.

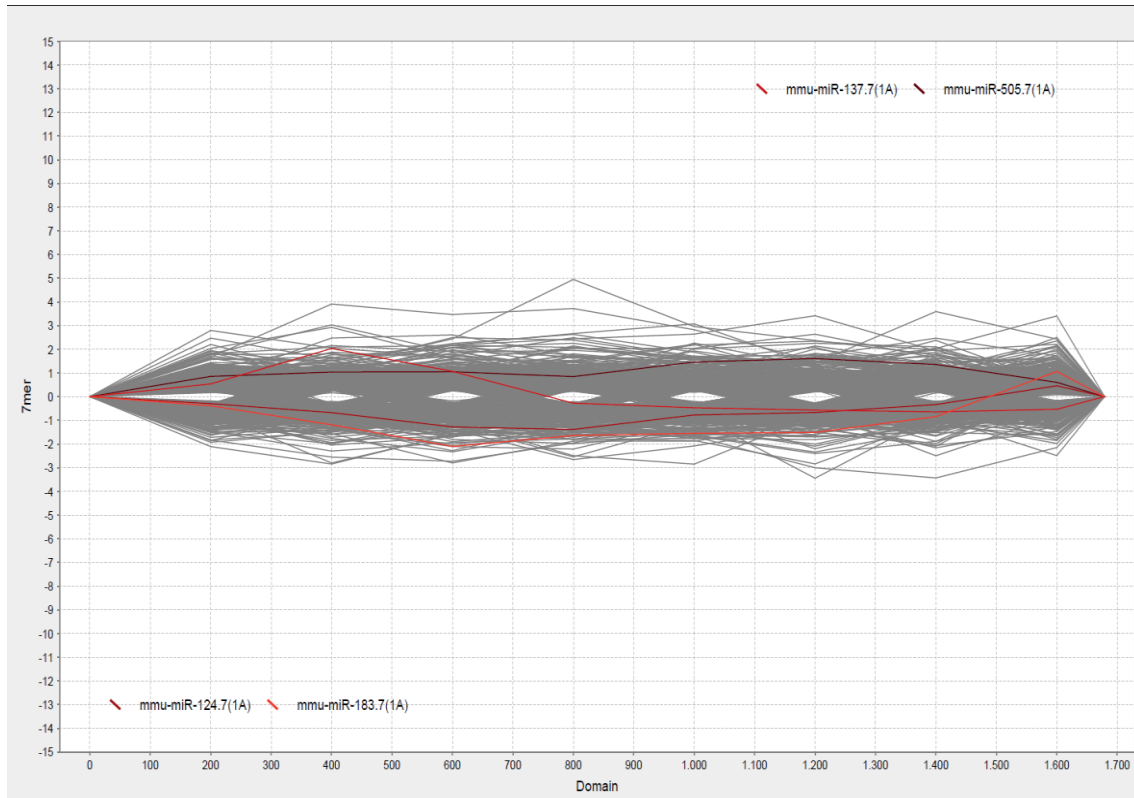


Figure 15: *SylArray* graph of wording regulation in damaged vs. contralateral DRG neurons. Genes are sorted by change in expression, in decreasing order. Y axis shows the log of enrichment/depletion p-value for 7-mer miRNA seeds in 3'UTR. Included are all miRNAs with a p-value of $p < 0.1$. Coloured lines represent putative candidate miRNAs miR-124, -137, -183, and -505.

Of the candidates in question, wordings consistent with miR-137, miR-183, and miR-505 showed significant regulation. The corresponding slopes, though, appear to lack a steep peak (**Fig. 15**). In the comparison between damaged and adjacent neurons, UTRs consistent with miR-125b-3p and -26a were most enriched, those matching miR-323-5p, -21, and -1933-5p displayed the strongest down-regulation (all $p < .01$). Still, again visualization did not show a distinctive pattern in relation to a specific subset of genes (**Fig. 16**).

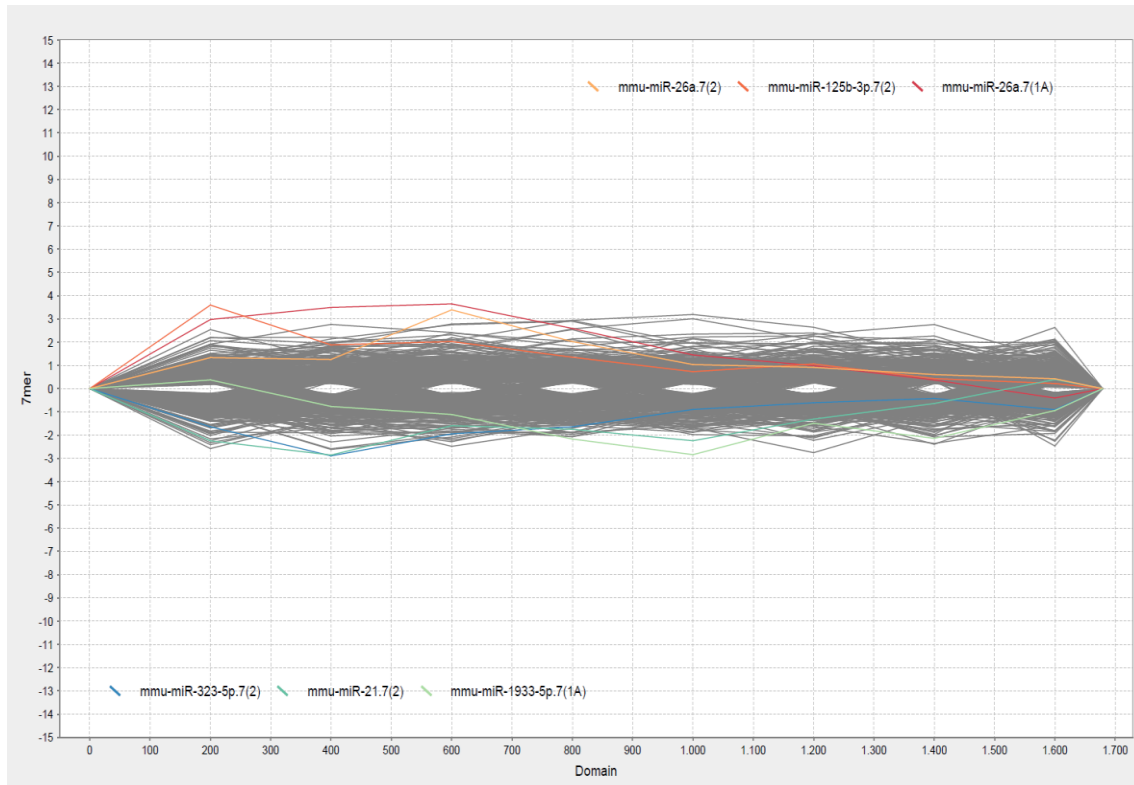


Figure 16: *SylArray* graph of wording regulation in damaged vs. adjacent DRG neurons. Genes are sorted by change in expression, in decreasing order. Y axis shows the log of enrichment/depletion p-value for 7-mer miRNA seeds in 3'UTR. Included are all miRNAs with a p-value of $p < 0.1$. Coloured lines represent the 6 most significant miRNA seeds.

Furthermore, for none of the aforementioned candidates wordings were enriched to a significant extent, consistent with flat slopes in the corresponding graph (**Fig. 17**). Findings and interpretation were confirmed through expert evaluation by developer Anton Enright (EBI, Hinxton).

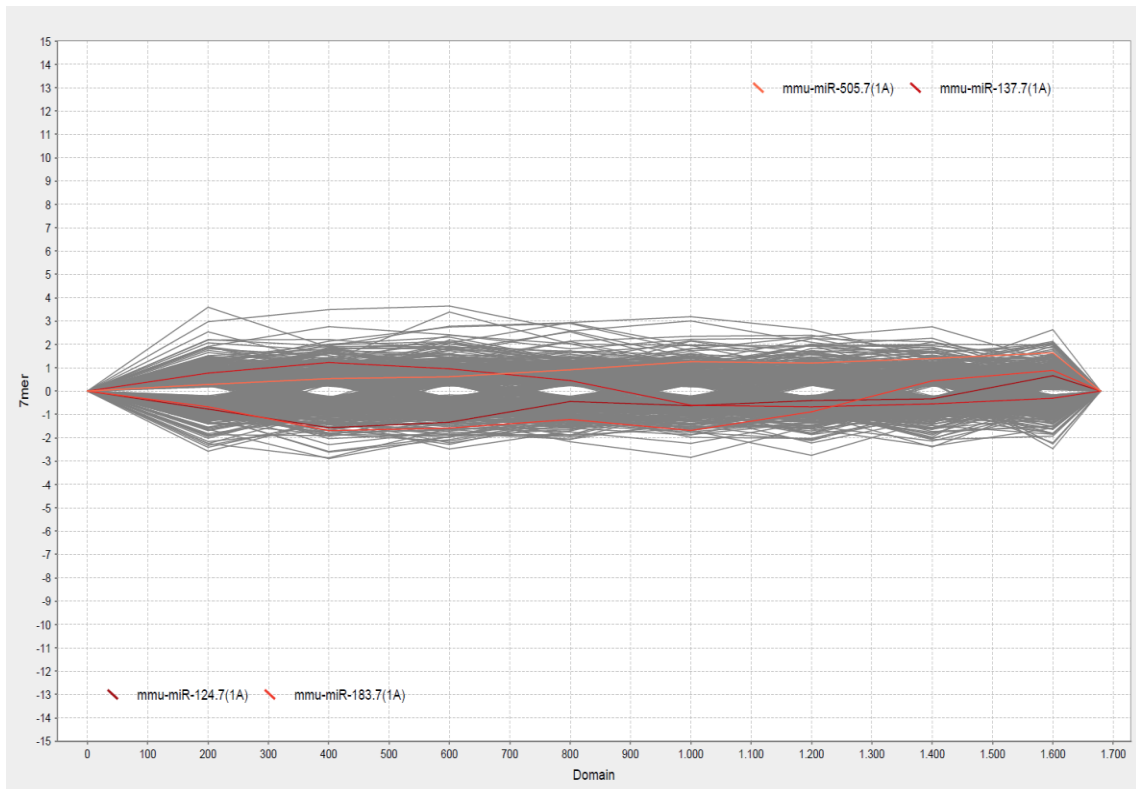


Figure 17: *SylArray* graph of wording regulation in damaged vs. adjacent DRG neurons. Genes are sorted by change in expression, in decreasing order. Y axis shows the log of enrichment/ depletion p-value for 7-mer miRNA seeds in 3'UTR. Included are all miRNAs with a p-value of $p < 0.1$. Coloured lines represent putative candidate miRNAs miR-124, -137, -183, and -505.

4.8.2 *MirAct* Analysis

Analysis of possible miRNA involvement included 143 miRNAs. Of these, 6 showed significant p-values ($p < .05$): let-7, miR-22, miR-361, miR-876-5p, miR-21, and miR-411. q-values were $>.3$ for any of them (see **table 12**. For discussion of p- vs. q-levels, cf. chapter 5.4.3).

	<i>p-value</i>	<i>q-value</i>
<i>let-7/98</i>	0.02732	0.3168
<i>miR-22</i>	0.02732	0.3168
<i>miR-361/361-5p</i>	0.02732	0.3168
<i>miR-876-5p</i>	0.03899	0.3168
<i>miR-21/590-5p</i>	0.03899	0.3168
<i>miR-411</i>	0.03899	0.3168

Table 12: *MirAct* analysis of gene expression results. MiRNAs most likely to be involved ($p < .05$).

For four out of the six miRNAs, putative targets were expressed highest in damaged neurons, followed by adjacent and contralateral neurons. The opposite is true for let-7. Only for miRNA 876-5p, expression levels of putative targets in damaged neurons are located between that of adjacent and contralateral neurons (**Fig. 18A-F**).

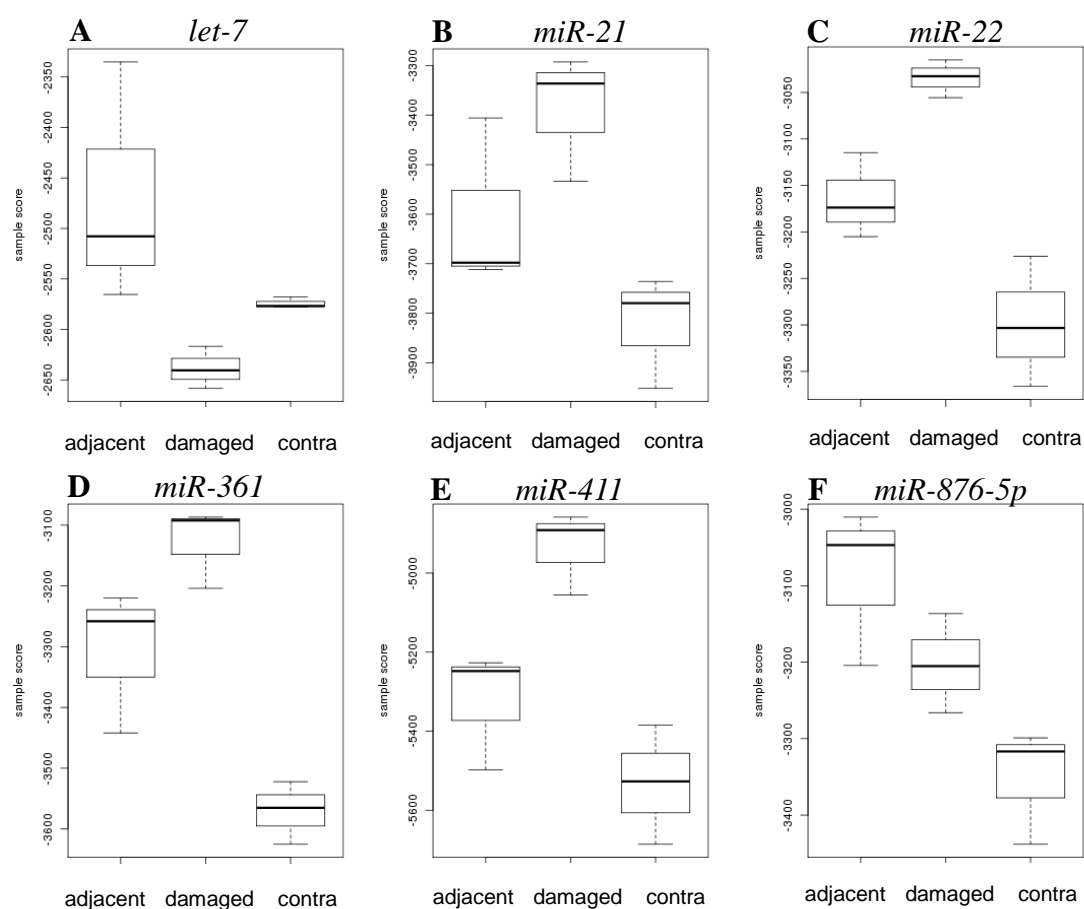


Figure 18: *MirAct* box plot of miRNAs with likely involvement (cf. table 12). Shown is suggested miRNA activity in damaged, adjacent, and contralateral DRG neurons (sample scores). Error bars indicate maximum and minimum values of 3 runs. With the exception of miR876-5p, findings suggest less extensive regulation in adjacent neurons. Note that the score corresponds to target activity, i.e. a higher score indicates low miRNA activity.

Of the previously identified candidates miRNAs, miR-137 was the most distinctive ($p=0.06646$; $q=0.3168$), followed by -183, -124, and, with some distance, miR-27b and -505 (see table 13, Fig. 19A-C).

	<i>p-value</i>	<i>q-value</i>
<i>miR-137</i>	0.06646	0.3168
<i>miR-183</i>	0.09915	0.3522
<i>miR-124</i>	0.09915	0.3522
<i>miR-27b</i>	0.28810	0.5722
<i>miR-505</i>	0.56114	0.7362

Table 13: *MirAct* analysis of gene expression. Results for miRNA candidates.

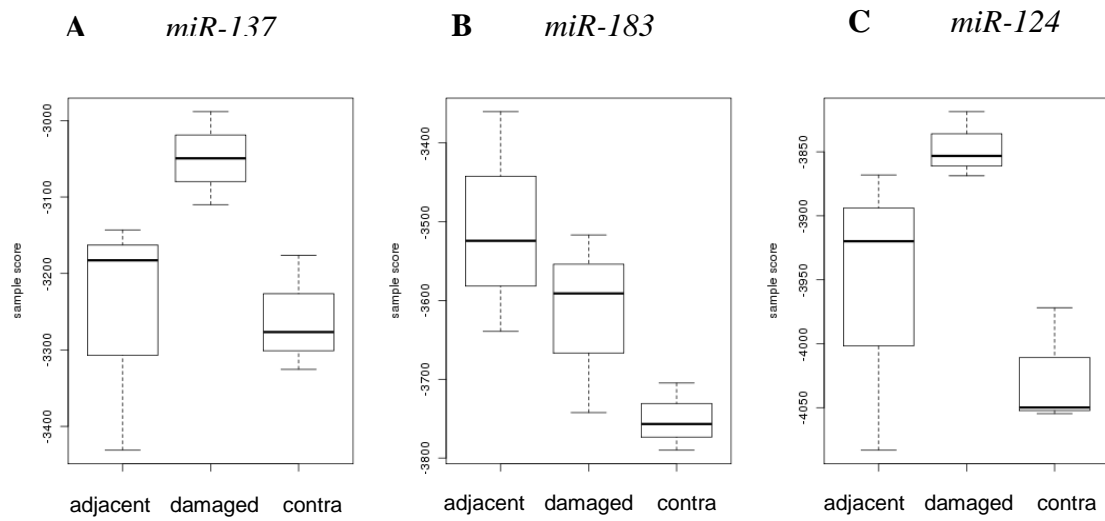


Figure 19: *MirAct* box plot of candidate miRNAs miR-137, -183, and -124 (cf. table 13). Shown is suggested miRNA activity in damaged, adjacent, and contralateral DRG neurons (sample scores). Error bars indicate maximum and minimum values of 3 runs. Note that the score corresponds to target activity, i.e. a higher score indicates low miRNA activity.

5 Discussion

5.1 MicroRNAs in Neuropathic Pain

The experiments presented aim to define a role for miRNAs in the development and regulation of neuropathic pain in mice. Changes in whole DRG were covered as well as in primary sensory neurons. Results suggest a contribution of miRNAs to neuropathic pain, singling out some in particular. Yet, the picture that emerges is varied and reflects the clinical and molecular complexity.

5.1.1 Time Course of microRNA Expression in DRG after CCI

After CCI surgery as performed in our group, a neuropathic phenotype typically evolves within the course of 7 d. This has been endorsed by a highly significant upregulation of galanin after 7 d. As miRNAs are known to interfere with mRNAs before gene translation, an earlier onset of miRNA differential expression had been hypothesized and different time points compared: 6 h, 1 d, and 7 d after CCI. In the assay data, differential regulation of miRNAs in DRG evolved over the time-course of 7 d: Ipsilateral samples after 7 d were most divergent from naïve controls. These findings are in accordance with other, later studies (Aldrich et al., 2009; Kusuda et al., 2011).

5.1.2 MicroRNA Profiling in Contralateral DRG

Notably, contralateral DRG exhibited a differential expression pattern as well, although to smaller extent. Thus, findings indicate a miRNA involvement both in local and systemic reactions to neuropathic agents. However, the relation between both, i.e. a thorough analysis of which miRNAs are involved exclusively in systemic processes and which have an additional side-specific effect, requires deeper research and must be further elucidated upon. As for now, no such investigation has been published yet.

5.2 MicroRNAs Potentially Involved in Neuropathic Pain

Initial whole-DRG screening did suggest several potential candidate miRNAs. For validation and quantification, five miRNAs were analysed using qPCR. Two of these were further characterized using *in situ* hybridization and bioinformatical target prediction.

5.2.1 A Potential Role for miR-183 in Various States of Pain

MiR-183, located on chromosome 6 and with a 22-nucleotide mature sequence, has been previously described as part of a sensory-organ specific cluster together with miR-96 and -182, notably in inner ear hair cells and in retinal neurons (Sacheli et al., 2009; Xu et al., 2007). *In silico* analysis of potential targets included genes known to be involved in neuropathic pain, such as voltage-gated ion channels (Nav1.3, Trek-1); proven targets include SRY-box containing gene 2 (Sox2) and Insulin receptor substrate 1 (Irs1) (Aldrich et al., 2009). As mentioned above, miR-183 has by now been described by two groups as being downregulated in inflammatory and neuropathic pain.

Both miRNA assay and PCR data showed a decreased expression of miR-183 in neuropathic DRG compared to controls as well as, to a lesser extent, contralateral DRG (**Table 3, Fig. 7A**). In PCR, expression was reduced by ~60% ipsi- and 20% contralaterally compared to naïve DRG. These findings are consistent with the report by Aldrich et al. who observed a downregulation of the sensory-organ specific cluster [miR-96, -182, -183] in rat DRG after spinal nerve ligation. In addition, the authors suggest an intracellular redistribution of miRNAs observed in *in situ* hybridization. Such alterations were not found for miR-183 in this study: signals were evenly distributed in the cytoplasm, also no consistent overall reduction was detectable. However, *in-situ* hybridisation is not a very sensitive method for gene expression quantification. (**Fig. 9**). Notably, no relevant regulation was found for other miRNAs of the suggested cluster, i.e. miR-96 and miR-182. This is in line with findings in inflammatory pain (Bai et al., 2007). As for potential target genes, the microarray did not show a strong differential expression of any of the suggested top targets. Rather, Trek-1, Sox-2, Nav1.3 and Irs-1 were slightly downregulated in our neuron-specific approach (not mentioned in table 9). Moreover, *in silico* analysis for miRNA involvement did not strongly suggest a role for miR-183 (in neither *SylArray* nor *MirAct*). Hence, at this point, no further conclusions can be made about the role of miR-183 in neuropathic pain from the data. Still, the consistency with previous data plus the ascribed role of miR-183 in sensory organs make it an interesting target for further research, especially in the light of upregulated genes of the inner ear like Otopetrin (see below).

5.2.2 miR-137 in Sensory Neurons and its Role in Pain

Mature miR-137 is formed by a 23-nucleotide long sequence, located on chromosome 3. It has not been pooled with other miRNAs into a functional cluster yet. Description focus primarily on malignant tumours, mainly colorectal carcinoma (Balaguer et al., 2010), uveal melanoma (Chen X et al., 2011) and squamous cell carcinoma of the head and neck (Langevin et al., 2011).

In the field of neuroscience, miR-137 is mainly described as an inhibitor of dendrite morphogenesis and spine development both *in vivo* and *in vitro* by targeting ubiquitin ligase mind-bomb1 Mib1, a regulator of neurogenesis (Smrt et al., 2010). Furthermore, Silber et al. observed a decreased expression of both miR-137 and miR-124 in glioblastoma multiforme and conclude a role for both in neural stem cell differentiation (Silber et al., 2008).

In this project, miR-137 was repeatedly downregulated in neuropathic pain, both ipsi- as well as contralaterally, although to various extents: In assay analysis, expression levels were similar on both sides, whereas qPCR analysis revealed strong side differences (**Fig. 7B**). Notably, *MirAct* analysis suggested an involvement of miR-137 in damaged neurons, compared to adjacent as well as contralateral neurons (**Fig. 19A**). Still, in all experiments, the observed changes were not significant due to high variance.

In situ hybridization/immunohistochemistry showed localization exclusively in small IB⁴⁺ DRG neurons, i.e. in non-peptidergic nociceptors (**Fig. 10**). Also, considering the findings by Silber et al., it is relevant to emphasize the neuron-specificity of the staining. Based on the findings, miR-137 in DRG can be regarded as nociceptor-specific with possible downregulation in neuropathic pain.

5.2.3 miR-124 in Pain – Neuronal or Immune Origin?

miR-124 is among the best-investigated miRNAs in the nervous system. Precursor forms are found on chromosomes 2, 11, and 14; its mature form consists of 20 nucleotides. Research ascribes a crucial role to it in neurogenesis and neuronal differentiation, in the central and peripheral nervous system alike (Makeyev et al., 2007). As mentioned above, decreased expression was shown after inflammatory pain (Bai et al., 2007). Initial assay findings on downregulation in neuropathic DRG could

not be repeated consistently in qPCR (**Fig. 8A**). *In silico* analysis for possible miRNA involvement in neuronal gene regulation did not yield explicit results, although *MirAct* analysis indicated a downregulation in damaged neurons (**Fig 19C**). While miR-124 has traditionally been regarded as neuron-specific, recent reports describe a role in immunoregulation: Ponomarev et al. (2011) observed a regulatory function in microglia and macrophages, while Soreq & Wolf (2011) regard it as part of a miRNA class responsible for neuroimmune interaction (*NeurimmiRs*). Bearing in mind that the only description of miR-124 in pain was in whole DRG after inflammation, it should be considered whether this effect might be explained by differential expression in peripheral immune cells rather than neurons: As described above, macrophage invasion constitutes a key element in chronic pain, but its extent might be subject to fluctuations and therefore account for the variations in whole-DRG results. Here, another cell-type-specific approach, e.g., co-staining with a macrophage-specific marker like CD68, might be helpful.

5.2.4 miR-505 and miR-27b

Only very little is known about miR-505 so far: It is described in breast cancer tissue, and a role in cell homeostasis by targeting splicing factor 2 has been suggested (Zhu et al., 2011). Results showed little consistency and could not be validated by quantitative methods. This might in part be due to low general expression levels as seen in the qPCR runs. Moreover, bioinformatical analysis of target expression (*MirAct*) does not suggest relevant activity. Thus, any conclusions about a contribution of miR-505 to neuropathic pain would be highly speculative.

MiR-27b has been repeatedly described in angiogenesis and vascular inflammatory processes (reviewed by Urbich et al., 2008) but also in malignant processes like glioma (Chen L et al., 2011). So far, it has not been mentioned in context with pain or peripheral neuronal processes. Recently, though, Thulangisam et al. (2011) suggested a role of miR-27b* (the antisense strand) in innate immune processes by targeting nuclear factor kB (NF-kB). As NF-kB positively regulates cyclooxygenase 2, an enzyme crucial in prostaglandin synthesis, a pro-nociceptive role would be plausible. Still, findings were not consistent and no inferences about a possible function of miR-27b in

neuropathic pain can be made from them.

Considering the striking similarity of graphs for miR-124, miR-27b, and miR-505 with the second run yielding higher amounts than the first run, it should be mentioned again that the denomination “run 1” and “run 2” is specific to each miRNA, i.e. runs for different miRNAs were performed at different times. Thus, a systemic error in one run (e.g. concerning the control sample) can be excluded.

5.2.5 Further microRNAs Described in Neuropathic Pain

When comparing the results of this project to findings from other groups, one has to take into account the different animal pain models used, from axotomy over loose nerve ligations (as used in this project) up to stress-inducing cell trituration. MiRNAs mentioned in literature as regulated in neuropathic pain include miR-1, -182, -183, -206, -21, -221, -500, -551b, and -96 (cf. chapter 1.4). Of these, only miR-1 and miR-183 showed a notable regulation in this experiment; the latter has already been covered above. MiR-1 expression was reduced >twofold in two assay runs, notably to the same degree ipsi- and contralaterally. Similar effects have been described after stress-inducing cell isolation and after nerve-ligation neuropathy (Bastian et al., 2010; Kusuda et al., 2011). In the neuron-specific microarray, on the other hand, no such cues were found for miR-1 involvement. Two points should be considered here: Most importantly, in the experiment, contralateral neurons serve as a control. In the whole-DRG approach, though, ipsi- and contralateral DRG exhibited a similar regulation of miR-1. In the aforementioned studies, contralateral controls were not included. Mir-1 downregulation might thus be a systematic effect. Moreover, Bastian et al.'s pain model is based on stress elicited by cell extraction. Although great care was taken to provide careful handling throughout the operations and keep mechanical stress to a minimum, the neuron-specific experiment is based on single-cell isolation, i.e. all conditions underwent this procedural step. In conclusion, miR-1 regulation might be a systemic stress response in neuropathic organisms.

MiR-21 has been described by Yu et al. (2011) and by Strickland et al. (2011) as an example of miRNA-induced neurite outgrowth regulation sciatic axotomy; it was found upregulated 7-fold after one week. In the CCI ligation model used here, it was not

impressively regulated. Yet, *MirAct* analysis for miR-21/590-5p did list it among the most significantly involved miRNAs: surprisingly, the respective graph shows an upregulation of putative targets, thus indicating a downregulation of miR-21 or -590-5p. Hence, miR-21 might be yet another example of contrary regulation in neurons after neuropathic vs deafferential pain.

No relevant differential expression can be noticed for miR-221, miR-500, miR-551b, or miR-206.

5.3 Divergent Results in microRNA Profiling

In general, the assessment of miRNA expression in DRG showed high divergence between different runs of the same experiment as well as between different experimental techniques (Luminex assay, qPCR, bioinformatical analysis)⁸.

One major obstacle lies certainly in experimental limitations. Per mouse and condition, only 3 DRG (L3-5) can be extracted. As (mi)RNA yield from DRG is meagre, this adds up to a considerable demand in animals. Moreover, this project was planned as preliminary investigation with limited budget. Thus, repetition options and thereby statistical interpretation were restricted. For the same reasons, no sham controls were included. With RNA pooled from several mice for each experimental run, individual effects are negligible. Still, technical effects need to be taken into consideration when interpreting results, e.g. trends in qPCR.

Considering literature findings, however, divergent and contradictory results seem to be a general phenomenon in the field: Only two miRNAs, miR-1 and miR-21, have been reported by more than one study. The divergent findings on this subject can be attributed to three major factors: the complexity of neuropathic pathways running simultaneously with antinociceptive and regenerative mechanisms, the modest extent of miRNA regulation, and the tissue heterogeneity in dorsal root ganglia. As the first two points are difficult to tackle in terms of experimental design, focus was subsequently laid on tissue composition: Whole-DRG approaches are established in the study of peripheral neuropathies. Still, one has to bear in mind the cellular heterogeneity of DRG: Studies suggest a neuronal percentage of only 15% of all DRG cells (Ng et al., 2010), the

⁸ As all experiments including surgery were conducted by the same person and under stable conditions, experimenter-dependent differences can be excluded as relevant factor.

largest part being made up by glia, i.e. Schwann and satellite cells. In fact, as described above, several DRG cell types are known to be involved in neuropathic mechanisms. As the proportions fluctuate across ganglia, cell-type-specific expression changes may vary considerably and, moreover, be drowned by high background signalling. In combination with the two other factors mentioned above, this might cause limitations in the investigation of miRNA-driven processes.

I therefore decided to take a cell type-specific approach by singling out neurons and comparing damaged vs. non-damaged neurons.

5.4 Neuron-Specific Expression Analysis

5.4.1 Advantages of Cell Type- and Damage-Specific Approach

As described above, the different properties of fluorescent neuronal tracers can be exploited to distinguish between neuronal subsets by double staining. However, so far this has mainly been used for histological experiments. By combining differential fluorescent neuronal labelling with fluorescence-activated cell sorting (FACS), the approach not only allows to study neuron-specific expression but also compare gene expression in damaged and adjacent intact DRG neurons. Thus, this neuron- and damage-specific approach better reflects previous findings (as reviewed by Campbell & Meyer, 2006) that emphasize different expression patterns in damaged and adjacent neurons as well as contributions of non-neuronal cells to neuropathic features.

As this design requires enormous amounts of primary tissue in order to yield enough final RNA for microarrays, some experimental features were adjusted to minimize consumption. These changes need to be taken into consideration when comparing the results to the initial whole-DRG approach: Firstly, as a control served contralateral DRG neurons instead of DRG neurons from naïve animals. Thus, comparisons are always made within the same animal; systemic reactions are therefore not captured. In previous experiments, contralateral neurons had exhibited altered expression, as well. Secondly, miRNA were not assessed directly: Instead, a mRNA microarray was performed and information about miRNA involvement inferred from *in silico* analysis. Beside the about tenfold decrease in RNA amount required and the more established principle, this approach served another purpose - mRNA information could be used as a quality control: Gene regulation in neuropathic sensory neurons has long been an extensively

researched field. Comparing results to literature served as validation for this rather novel approach.

5.4.2 mRNA Regulation in Damaged Neurons

5.4.2.1 Global Findings

The FACS pattern for ipsilateral neurons consistently uncovered a subpopulation of DiI⁺/FE⁺ cells, suggesting strong neuronal damage. The bulk of cells negative for both DiI and FE reaffirms the high amount of non-neuronal tissue in DRG. As correlation and Principal Component Analysis both show a high consistency within damaged and contralateral neurons respectively, this approach can be assumed effective. Interestingly, this consistency is not the case true for non-damaged neurons; this observation might be caused by anatomical differences (projection from peripheral to spinal nerves differs considerably between individuals: While all DRG L3-L5 are used for the study of sciatic pain models, the bulk of the sciatic nerve actually projects into L4 (Rigaud et al., 2007)).

In mRNA analysis, the number of genes differentially regulated compared to other conditions was by far the highest for damaged neurons. Interestingly, the vast majority of the genes showed a regulation in damaged neurons that was considerably bigger compared to contralateral than to adjacent neurons. This gives the latter an “intermediate” position thus indicating a trickle-down or paracrine-like effect. Such changes in neighbouring tissue are in line with previous descriptions (e.g., reviewed by Campbell & Meyer, 2006). Yet, some genes presented the contrary, thus indicating a regulation exclusively in adjacent neurons. These include zinc finger, transmembrane or gap junction proteins. Yet, differential regulation is only marginal.

Results show quantitative differences between FACS runs. These considerable within-group variations can be attributed to different yields in cell extraction as well as diverging efficiency of tracer injection. Moreover, they appear to confirm the aforementioned concerns of individual composition differences in DRG tissue.

As this thesis is chiefly concerned with the regulation of miRNAs, a thorough analysis of gene expression findings would be beyond the scope. The following discussion will

therefore focus on structures known to be regulated which might hence serve as quality control, and only glance at some surprising and highly interesting novel genes, such as CRH (see below).

5.4.2.2 Regulation of Genes Described in Neuropathic Pain

In the microarray, a number of genes known to play a role in neuropathic pain have been differentially upregulated (Table 8). Among them are several **ion channels**: ATP-sensing purinergic receptor P2rx3 has been long considered one of the major factors in neuronal sensitization, as has calcium channel subunit $\alpha 2\delta 1$, the target of Gabapentin (Ji & Strichartz, 2004). Also L-type calcium channel $Ca_v 1.2$, a regulator of the CREB pathway, has been described in neuropathic pain. Surprisingly, voltage-gated M-type potassium channel Kcnq2, responsible for maintenance of resting membrane potential, was upregulated in the experiment. This is contrary to literature findings (e.g. Rose et al., 2011). Moreover, analgesics like flupirtine are known to act as Kcnq2 activators (Gribkoff, 2003).

Channels down-regulated include various potassium channels (e.g. Kcnj10, Kcnn4, Kctd1; see table 9). Voltage-gated potassium channel Kcnk2 (TREK-1) has been described as polymodal pain sensor in small sensory neurons, regulated by GPCRs and co-localized with TRPV1. Interestingly, mice with a disrupted TREK-1 gene are more prone to thermal hyperalgesia (Alloui et al., 2005). Also Kcnc4 has been reported to be reduced in neuropathic sensory neurons, thereby causing mechanical hypersensitivity (Chien et al., 2007). At the same time, a number of voltage-gated sodium channels are downregulated, among them $Na_v 1.1$ and TTX-R $Na_v 1.8$ and 1.9. Especially the role of $Na_v 1.8$ in pain is still under debate. Still, it has, like $Na_v 1.9$, been described as being down-regulated in perikarya of injured neurons but to accumulate in adjacent axons (Lampert et al., 2010; Ji & Strichartz, 2004). Notably, two transient receptor potential channels are among the downregulated genes, Trpm3 and Trpa1, which is in accordance with findings from Staaf et al. (2009) and Caspani et al (2009).

Of “classical” **neuropeptides** known to be involved in neuropathic pain, only some met ANOVA inclusion criteria. Most notable are galanin and its receptor Gpr151. Their

upregulation in damaged and, to lesser extent, in adjacent neurons is concordant with previous findings (Ma & Bisby, 1997). Other examples include neurotensin and cholecystokinin (CCK) which are thought to form a descending facilitatory pathway in the management of pain: Gui et al. (2004) describe a facilitation of visceral nociception by neurotensin that can be blocked by administration of CCK antagonists. Interestingly, higher concentrations of neurotensin seem to have an antinociceptive effect. Both phenomena have been described a) for nociceptive pain and b) in the spinal cord. Nevertheless, the upregulation of both neurotensin and CCK receptor B observed here, should be evaluated in the light of these findings. Further research into their role in peripheral neuropathic pain seems therefore promising. Chemokine CCL2 has been described as inflammatory and pain mediator released from primary afferents in the dorsal horn spinal cord. It is co-localized with classical “neuropathic” peptides like substance P and CGRP and thought to potentiate glutamergic receptors (AMPA/NMDA) as well as inhibit GABAergic receptors (GABA_A) (cf. Van Steenwinckel et al., 2011).

The fact that neuropeptide Y and CGRP were excluded from ANOVA due to inconsistent expression seems surprising. Yet, raw data, do point towards an upregulation of NPY and downregulation of CGRP in damaged neurons - which is consistent with data in literature (Shi et al., 2001).

CD38 is an ADP ribosylcyclase that regulates transmembrane Ca²⁺ flux. An explicit regulation in pain has not been described yet, but it has been shown to serve an antinociceptive function through μ -opioid receptor regulation (Hull et al., 2010).

Further genes highly upregulated encode for proteins involved in axonal growth and neuronal differentiation, like Syndecan1, growth factor Fgf3, Kainate-receptor modulator Neto1, aminotransferase Bcat1, AMPAR-associated Shisa9 or Sox (SRY box-containing gene) 11. Chac1 and Ecel1 are known to act downstream transcription factor Atf3, a marker of neuronal damage (Tsujino et al., 2000). Another group of upregulated genes hint at the inflammatory component of neuropathic pain, e.g. several CC chemokines, seizure-related gene 6, peptidase inhibitor Serpinb1a, or Annexin 1. Among the most down-regulated genes is Brevican, a chondroitin sulphate proteoglycan with growth-inhibiting features. In neuropathies, it has previously been described as up-regulated in dorsal root injury, i.e. deafferentiation (Waselle et al., 2009). As many of

these regulations are also found between damaged and adjacent neurons, underlines the importance of not only a cell type-specific approach but also a differentiation of bystanders. This is particularly true for Corticotropin-releasing hormone (CRH).

Most remarkably, **CRH**, starting point of the hypothalamic-pituitary-adrenal (HPA) axis, was upregulated more than 200-fold compared to contralateral and 19-fold compared to adjacent neurons (not shown in table). The role of CRH and its receptors (CRH-R1 and CRH-R2) in neuropathy has not yet been well-defined. So far, two working mechanisms have been proposed: endogenous analgesia and nerve regeneration. In animal models, neuropathic pain can be alleviated by direct application of CRH to the nerve. As in inflammatory pain, this is caused by release of opioid peptides from infiltrating leukocytes. The analgesic effect can be antagonised by application of naloxone (Labuz, 2009). However, little has been found yet as to which cells express endogenous CRH in neuropathy. In the periphery, an increased expression of CRH and its receptors has mainly been shown in immune cells (Mousa, 2007). Moreover, a co-overexpression of CRH with pain-relevant neuropeptides has been observed in DRG and nociceptors (Skofitsch, 1985). Another hypothesis suggests a role in nerve regeneration by releasing brain-derived neurotrophic factor (BDNF) and promoting axonal outgrowth (Yuan, 2010). Neuronal CRH expression has been described mainly in the hypothalamus (Aguilera & Liu, 2011): only little is known about its role in the peripheral nervous system. Kim EH et al. (2010) showed an increased immunoreactivity of CRH and its receptors in contralateral DRG after deafferentation pain in rats. The differential neuron-specific approach of this experiment showed for the first time an upregulation in primarily damaged DRG neurons as well as, to a lesser extent, in their intact bystanders compared to contralateral DRG neurons. This suggests a central role for local neuronal CRH in neuropathic pain. Notably, the regulation of CRH does not seem to be part of an altered HPA responsiveness to a painful stressor: Bomholt et al. (2005) evidenced a normal HPA function in the CCI model. Thus, CRH seems to be an interesting and still under-investigated player in neuropathic pain. *In silico* analysis suggested several miRNAs involved in CRH regulation, e.g. miR-486, miR-881, miR-494, or miR-669d (miRWalk (<http://www.umm.uni-heidelberg.de/apps/zmf/mirwalk/>, last retrieved June, 20th, 2014) (Dweep et al. 2011).

However, none of these has yet been linked to CRH in experiments, nor have they been considerably regulated in our experiments.

To further elucidate the role of CRH, e.g. as analgesic agent or as promoter of axonal regeneration, a conditional knock-out animal is being developed. The example of CRH underlines the merits of the differential fluorescent tracing model presented here. Not only allows this cell type-specific approach a more detailed insight into gene regulation than a whole DRG screening. Moreover, the separation of primarily damaged and adjacent intact DRG neurons crucial towards a further understanding and functional characterization of hitherto often under-investigated “innocent bystanders” and the importance of interaction between these two groups.

Given the high congruence with literature data and the repeated reference to nociceptive/neuropathic pathways, it is sound to conclude that this experimental approach was successful.

5.4.2.3 Novel Regulated Genes

Differential expression was detected including in genes hitherto not described in relation with pain.

Otopetrin 1 (Otop1) is a multi-transmembrane domain protein that has been mainly described in vestibular supporting cells. There, it regulates intracellular Ca^{2+} concentration by modifying purinergic receptor activity, mainly by enhancing ATP-gated channel P2xr (Kim E et al., 2010). As P2xr is a crucial factor in the neuropathic cascade, a hypothetical role of Otop1 in neuropathic pain is reasonable. As it has not yet been described in this context, though, a further exploration of its function would therefore be highly interesting.

Furthermore, several ion channels that were regulated in the experiment have not been described in neuropathic pain before. Yet, their properties and known functions make a role in neuropathy plausible. For example, inward rectifying two-pore-domain-potassium channel Kcnk6 is activated by protein kinase C (Lesage & Lazdunski, 2000). Kctd12 is an inward-rectifying potassium channel expressed mainly in the CNS and the inner ear that forms part of GABA(B) receptors (Schwenk et al., 2010). Further research on these channels in pain might be interesting, as well as for anoctamin 4, a calcium-

activated chloride channel of the Tmem16 family, and Hvcn1, a voltage-gated proton channel.

5.4.3 Bioinformatical Inference on Potential microRNA Contribution

Bioinformatical strategies to predict miRNA-mRNA relations have seen an enormous development throughout the past years which goes far beyond mere sequence comparison.

Despite greatly improved algorithms, though, their reliability and especially specificity are still highly disputed. Most databases still offer large lists of possible targets: The number often goes into the hundreds or thousands. This is not surprising, taking into account the length of many mRNAs and the small size of the seed region. Hence, for analysis of mRNA expression data for miRNA involvement two different algorithms, *SylArray* and *MirAct*, were used .

Despite some differences, neither one found strong evidence for a specific miRNA. *SylArray* curves do not hint at any miRNA in particular, especially none of the previous candidates, miR-137 or -183: Though significance levels ($<.01$) are obtained, the small variation of enrichment along the gene list is not suggestive of specific gene targeting.

MirAct emits two different measures of significance, the established p-value and the novel q-value which is based on the false discovery rate. As it is more resistant to repetitive testing, it is by now widely used in whole genome arrays. Still, as p-value prevails as a parameter, both are included in this analysis. Based on a p-value <0.05 , six miRNAs show significant regulation in neuropathic sensory neurons. One of these, miR-21, has been mentioned in a previous study. Notably, miR-137, miR-183, and miR-124 are suggested as having a considerable effect, though not significant ($p<0.1$). In this context, it is interesting to see the different regulation patterns for the various miRNAs: While miR-137 seems to be most important in damaged neurons followed by their adjacent; the opposite is true for miR-183. Still, relying on the q-value, no single miRNA is predicted to be involved in neuropathic regulation.

Lack of significant miRNA results in both *in silico* approaches might arise from four reasons (besides multiple testing problem): Firstly, such subtle regulation of miRNA as assumed from previous experiments might reflect only poorly in bioinformatical analysis: Most “sample” analyses had been made with knockout experiments or *ex post*

with data that had already evidenced the strong regulation of one single miRNA (cf. Bartonicek & Enright, 2010). Secondly, neuropathic pain has been shown to consist of a complex interaction of different molecular mechanisms: In many of them, miRNAs might be only of minor importance and their effect therefore drowned by other relevant alterations. Thirdly, miRNAs are often upstream a multifactorial cascade, e.g. they might regulate transcription factors. It would thus be not its direct targets that are regulated the most, and tracing back from highly upregulated genes to matching miRNA seeds would not be possible. MiR-137, for example, has been argued as evidence in favour of the multi-hit theory of carcinogenesis (cf. Balaguer et al., 2010). In line with these considerations, Baek et al (2008) found several miRNAs targeting the same mRNAs and regard single miRNAs rather as “fine-scale adjusters” in protein regulation. Implications for bioinformatical approaches are described by Liang et al (2011b). Last, but not least, one must keep in mind that, unlike the previous whole-DRG experiment, this approach assessed only neurons. Yet, a crucial role of non-neuronal, foremost glial tissue in the development and maintenance of neuropathic pain has been widely accepted in the scientific community by now (Marchand et al., 2005; Scholz & Woolf, 2007; Ohara et al., 2009). On the other hand, miRNA have an accepted role in inflammatory processes (e.g., McCoy, 2011). Bearing these facts in mind, a similar investigation of miRNA in specific non-neuronal cell-types, e.g. glia, would be desirable.

5.5 Outlook

Thanks to the various approaches in detecting novel mechanisms in neuropathic pain, there are several strands of research that merit further investigation: On a miRNA level, a further characterization of miR-183 and 137 might lead to new insights. Next, as gene expression data displayed, there still seem to be under-investigated players in neuropathic pain, like CRH or Otop1. Finally, on a structural level, the idea of a cell-type-specific approach seems promising and should be extended e.g., to glial tissue. In general, for further studies it would be desirable to link gene regulation to behavioural data, i.e. by assessing the neuropathic phenotype of operated mice.

5.5.1 Validation of miR-183 and -137 in Neuropathic Pain

The next step in defining the role of miR-183 and -137 in neuropathic pain would be *in-vivo* testing. Yet considering the complex and heterogeneous mechanisms underlying the emergence of pain, manipulation of a single miRNA would scarcely lead to measurable changes in phenotype. (If at all, extreme mimicking might lead to some induction of neuropathic pain-like behaviour in non-injured mice.) Rather, it might be more promising to further narrow down potential targets, be it experimentally, like HITS-CLIP (*high-throughput sequencing of RNAs isolated by crosslinking immunoprecipitation*, cf. Licatalosi, 2008) or with further refined bioinformatical methods. Based on this, potential pathways might be developed and their role be further defined by manipulating the entire pathway instead of a single regulatory unit.

5.5.2 Further Characterisation of Specific Genes in Neuropathic Pain

The results displayed a distinctive expression pattern of several genes little or not at all described in relation to neuropathic pain until now. Among the most striking ones is certainly corticoliberin (CRH) which exhibits features similar to other peptides like galanin, substance P, and vasoactive intestinal peptide (VIP). First follow-up experiments within our work group seem to confirm the results (Reinhold et al., submitted); *in-vivo* studies including transgenic approaches are in progress.

Also, the role of calcium-regulating Otop1 deserves further investigation: Its effect via purinergic P2X receptors renders the peptide highly interesting, as does the topical relation to miR-183 in the vestibular inner ear. Immunohistochemistry in control vs. neuropathic tissue might endorse the findings presented here. Also, a quantitative assessment of Otop1 after miRNA-183 silencing might offer further insight. Again, *in-vivo* silencing or mimicking of Otop1 is challenging not only for the complexity of neuropathic phenotypes but also for the global relevance of its most relevant target, P2XR: As it is crucial not only for neuropathic conditions, a highly distorted phenotype is to be expected.

5.5.3 Cell Type-Specific Expression Analysis

Given the diversity in cellular composition of DRG and the neuron-specific results presented here, the concept of cell type-specific analysis seems promising. A similar

approach for glial tissue, i.e. satellite cells ipsi- and contralaterally is conceivable. Yet, one has to bear in mind that satellite cells are mainly involved in inflammatory processes of neuropathic pain: therefore, phenotypic testing would be necessary here to rule out mere inflammation due to an invasive and potentially infectious procedure (as an alternative, pain parameters could be measured in neuronal populations).

Also, it would be interesting to repeat the neuron-specific approach with a miRNA microarray or with naïve animals as negative controls. Still, both approaches would require considerably higher amounts of RNA and therefore primary tissue, if conducted in mice.

6 Summary/Zusammenfassung

6.1 Summary

Neuropathic pain, caused by neuronal damage, is a severely impairing mostly chronic condition. Its underlying molecular mechanisms have not yet been thoroughly understood in their variety. In this doctoral thesis, I investigated the role of microRNAs (miRNAs) in a murine model of peripheral neuropathic pain. MiRNAs are small, non-coding RNAs known to play a crucial role in post-transcriptional gene regulation, mainly in cell proliferation and differentiation. Initially, expression patterns in affected dorsal root ganglia (DRG) at different time points after setting a peripheral nerve lesion were studied. DRG showed an increasingly differential expression pattern over the course of one week. Interestingly, a similar effect, albeit to a smaller extent, was observed in corresponding contralateral ganglia. Five miRNA (miR-124, miR-137, miR-183, miR-27b, and miR-505) were further analysed. qPCR, *in situ* hybridization, and bioinformatical analysis point towards a role for miR-137 and -183 in neuropathic pain as both were downregulated. Furthermore, miR-137 is shown to be specific for non-peptidergic non-myelinated nociceptors (C fibres) in DRG. As the ganglia consist of highly heterocellular tissue, I also developed a neuron-specific approach. Primarily damaged neurons were separated from intact adjacent neurons using fluorescence-activated cell-sorting and their gene expression pattern was analysed using a microarray. Thereby, not only were information obtained about mRNA expression in both groups but, by bioinformatical tools, also inferences on miRNA involvement. The general expression pattern was consistent with previous findings. Still, several genes were found differentially expressed that had not been described in this context before. Among these are corticoliberin or cation-regulating proteins like Otopetrin1. Bioinformatical data conformed, in part, to results from whole DRG, e.g. they implied a down-regulation of miR-124, -137, and -183. However, these results were not significant.

In summary, I found that a) miRNA expression in DRG is influenced by nerve lesions typical of neuropathic pain and that b) these changes develop simultaneously to over-expression of galanin, a marker for neuronal damage. Furthermore, several miRNAs (miR-183, -137) exhibit distinct expression patterns in whole-DRG as well as in neuron-specific approaches. Therefore, further investigation of their possible role in initiation and maintenance of neuropathic pain seems promising.

Finally, the differential expression of genes like Corticoliberin or Otopetrin 1, previously not described in neuropathic pain, has already resulted in follow-up projects.

6.2 Zusammenfassung

Neuropathischer Schmerz, d.h. Schmerz durch neuronale Schäden, ist eine stark beeinträchtigendes, oft chronisches Leiden. Die hierfür verantwortlichen molekularen Geschehen sind in ihrer Breite bislang nur unzureichend verstanden. In meiner Promotion habe ich die Rolle von microRNAs (miRNAs) in einem Mäusemodell des peripheren neuropathischen Schmerzes untersucht. MiRNAs sind kleine, nicht kodierende RNAs, die für posttranskriptionelle Genregulation, besonders Zellproliferation und –differenzierung verantwortlich sind. Im Experiment wurde zunächst ihre Expression in den Dorsalganglien geschädigter Nerven analysiert. Hier zeigte sich im Verlauf einer Woche ein zunehmend differentielleres Expressionsmuster. Bemerkenswert war ein ähnlicher, wenn auch geringerer Effekt in kontralateralen Ganglien. In einem weiteren Schritt wurden fünf ausgewählte miRNAs (miR-124, miR-137, miR-183, miR-27b und miR-505) weiter analysiert. qPCR, *In-situ*-Hybridisierung und bioinformatische Untersuchungen deuteten auf Mindereexpression von miR-137 und -183 bei neuropathischem Schmerz hin. Weiterhin stellte sich miR-137 als spezifisch für nicht-peptiderge nicht-myelinisierte Nozizeptoren in Dorsalganglien heraus. Da Dorsalganglien aus äußerst heterozellulärem Gewebe bestehen, entwickelte ich im Folgenden einen neuronenspezifischen Ansatz: Primär geschädigte sowie intakte benachbarte Neuronen wurden durch fluoreszenzaktivierte Zellsortierung (FACS) selektiert und ihre Genexpression jeweils in einem Microarray analysiert. Hierdurch konnten nicht nur direkte Informationen über mRNA-Expression in beiden Gruppen gewonnen, sondern durch bioinformatische Techniken auch Rückschlüsse auf miRNA-Expression gezogen werden. Das generelle Expressionsmuster entsprach der einschlägigen Literatur, allerdings zeigten sich auch bislang nicht beschriebene Veränderungen. Hierzu gehören Corticoliberin sowie Otopetrin1. Die bioinformatische Analyse bestätigte teilweise die Ergebnisse aus der ersten, ganglienweiten Untersuchung: Sie wiesen auf eine Mindereexpression von miR-124, -137 und -183 hin, allerdings waren diese Ergebnisse nicht signifikant.

Zusammengefasst zeigte sich, dass sich a) die Expression von miRNA in Dorsalganglien nach neuropathischen Läsionen ändert, und b) diese Veränderungen parallel zum neuropathischen Phänotyp entwickeln. Weiterhin wiesen mehrere miRNAs

markante Expressionsmuster sowohl in ganglienweiten wie in neuronenspezifischen Untersuchungen auf. Daher scheint die weitere Untersuchung ihrer Rolle in Entwicklung und Aufrechterhaltung von neuropathischem Schmerz vielversprechend. Schließlich hat die Entdeckung von Expressionsveränderungen bei Genen wie Corticoliberin und Otopetrin1, bislang nicht im Zusammenhang mit neuropathischem Schmerz beschrieben, bereits zu Nachfolgeprojekten geführt.

7 Bibliography

- Aguilera G & Liu Y (2012). The molecular physiology of CRH neurons. Front Neuroendocrinol **33**(1): 67-84.
- Aldrich BT, Frakes EP, Kasuya J, et al. (2009). Changes in expression of sensory organ-specific microRNAs in rat dorsal root ganglia in association with mechanical hypersensitivity induced by spinal nerve ligation. Neuroscience **164**(2): 711-723.
- Alloui A, Zimmermann K, Mamet J, et al. (2006). TreK-1, a K⁺ channel involved in polymodal pain perception. EMBO J **25**: 2368-2376.
- Attal N, Cruccu G, Haanpaa M, et al. (2006). EFNS guidelines on pharmacological treatment of neuropathic pain. Eur J Neurol **13**(11): 1153-1169.
- Bähr M & Frotscher M (2003). Duus' Neurologisch-topische Diagnostik. Stuttgart, Georg Thieme Verlag.
- Baek D, Villén J, Shin C, et al. (2008). The impact of microRNAs on protein output. Nature **455**(7209): 64-71.
- Baek J, Kang S, Min H (2014). MicroRNA-targeting therapeutics for hepatitis C. Arch Pharm Res **37**(3): 299-305.
- Bai G, Ambalavanar R, Wei D, et al. (2007). Downregulation of selective microRNAs in trigeminal ganglion neurons following inflammatory muscle pain. Mol Pain **3**: 15.
- Balaguer F, Link A, Lozano JJ, et al. (2010). Epigenetic silencing of miR-137 is an early event in colorectal carcinogenesis. Tumor and Stem Cell Biology **70**(16).
- Baron R (2006). Mechanisms of disease: neuropathic pain - a clinical perspective. Nat Clin Pract Neurol **2**(2): 95-106.
- Bartel DP (2009). MicroRNAs: target recognition and regulatory functions. Cell **136**(2): 215-233.
- Bartonicek N & Enright AJ (2010). SylArray: a web server for automated detection of miRNA effects from expression data. Bioinformatics **26**(22): 2900-2901.
- Bastian I, Tam Tam S, Zhou XF, et al. (2011). Differential expression of microRNA-1 in dorsal root ganglion neurons. Histochem Cell Biol **135**(1): 37-45.
- Bennett GJ & Xie YK (1988). A peripheral mononeuropathy in rat that produces disorders of pain sensation like those seen in man. Pain **33**(1): 87-107.
- Bennett GJ (1998). Neuropathic pain: new insights, new interventions. Hosp Pract (Minneapolis) **33**(10): 95-98.
- Berger A, Dukes EM & Oster G (2004). Clinical characteristics and economic costs of patients with painful neuropathic disorders. J Pain **5**(3): 143-149.
- Blenkiron C, Goldstein LD, Thorne NP, et al. (2007). MicroRNA expression profiling of human breast cancer identifies new markers of tumor subtype. Genome Biol **8**(10): R214.
- Bomholt SF, Mikkelsen JD & Blackburn-Munro G (2005). Normal hypothalamo-pituitary-adrenal axis function in a rat model of peripheral neuropathic pain. Brain Res **1044**: 216-226.
- Bonica JJ (1979). The need of a taxonomy. Pain **6**(3): 247-8.
- Boucher TJ & McMahon SB (2001). Neurotrophic factors and neuropathic pain. Curr Opin Pharmacol **1**(1): 66-72.
- Campbell JN & Meyer RA (2006). Mechanisms of neuropathic pain. Neuron **52**(1): 77-92.

- Caspani O, Zurborg S, Labuz D, et al. (2009). The contribution of TRPM8 and TRPA1 channels to cold allodynia and neuropathic pain. PLoS One **4**(10): e7383.
- Caterina MJ & Julius D (1999). Sense and specificity: a molecular identity for nociceptors. Curr Opin Neurobiol **9**(5): 525-530.
- Chen X, Wang J, Shen H, et al. (2011). Epigenetics, MicroRNAs, and Carcinogenesis: Functional role of microRNA-137 in uveal melanoma. Invest Ophthalmol Vis Sci **52**(3): 1193-1199.
- Chen L, Li H, Han L, et al. (2011). Expression and function of miR-27b in human glioma. Oncol Rep **26**(6): 1617-1621.
- Cheng C, Wang Q, You W, et al. MiRNAs as biomarkers of myocardial infarction. A meta-analysis. PloS One **9**(2):e88566
- Chien LY, Cheng JK, Chu D, et al. (2007). Reduced expression of A-type potassium channels in primary sensory neurons induces mechanical hypersensitivity. J Neurosci **27**(37): 9855-9865.
- Choi D, Li D & Raisman G (2002). Fluorescent retrograde neuronal tracers that label the rat facial nucleus: a comparison of Fast Blue, Fluoro-ruby, Fluoro-emerald, Fluoro-Gold and DiI. J Neurosci Methods **117**(2): 167-172.
- Chu AS & Friedman JR (2008). A role for microRNA in cystic liver and kidney diseases. J Clin Invest **118**(11): 3585-3587.
- Closs SJ, Staples V, Reid I, et al. (2009). The impact of neuropathic pain on relationships. J Adv Nurs **65**(2): 402-411.
- Corrada D, Viti F, Merelli I, et al. (2011). myMIR: a genome-wide microRNA targets identification and annotation tool. Briefings in Bioinformatics **12**(6): 588-600.
- Davis-Dusenbery BN & Hata A (2010). Mechanisms of control in microRNA biogenesis. J Biochem **148**(4): 381-392.
- Dray A (2008). Neuropathic pain: emerging treatments. Br J Anaesth **101**(1): 48-58.
- Dweep H, Sticht C, Pandey P, et al. (2011). miRWalk-database: prediction of possible miRNA binding sites by “walking” the genes of three genomes. J Biomed Inform **44**(5):839-47.
- Dworkin RH, O'Connor AB, Backonja M, et al. (2007). Pharmacologic management of neuropathic pain: evidence-based recommendations. Pain **132**(3): 237-251.
- Ekberg J & Adams DJ (2006). Neuronal voltage-gated sodium channel subtypes: key roles in inflammatory and neuropathic pain. Int J Biochem Cell Biol. **38**(12): 2005-2010.
- Ferrante FM & VadeBoncouer TR (1993). Postoperative pain management. New York, Churchill Livingstone.
- Fritzschn B & Sonntag R (1991). Sequential double labelling with different fluorescent dyes coupled to dextran amines as a tool to estimate the accuracy of tracer application and of regeneration. J Neurosci Methods **39**(1): 9-17.
- Gribkoff VK (2003). the therapeutic potential of neuronal KCNQ channel modulators. Exp Opin Ther Targets **7**(6): 737-748.
- Guarnieri DJ & DiLeone RJ (2008). MicroRNAs: a new class of gene regulators. Ann Med **40**(3): 197-208.
- Gui X, Carraway RE & Dobner PR (2004). Endogenous Neurotensin facilitates visceral nociception and is required for stress-induced antinociception in mice and rats. Neuroscience **126**: 1023-1032.
- He L & Hannon GJ (2004). MicroRNAs: Small RNAs with a big role in gene regulation. Nat Rev Genet **5**(7): 522-531.

- Honig MG & Hume RI (1986). Fluorescent carbocyanine dyes allow living neurons of identified origin to be studied in long-term cultures. J Cell Biol **103**(1): 171-187.
- Hull LC, Rabender C, Bichoy HG, et al. (2010). Role of CD38, a cyclic ADP-ribosylcyclase, in morphine antinociception and tolerance. J Pharmacol Exp Ther **334**(3): 1042-1050.
- Iorio MV, Visone R, Di Leva G, et al. (2007). MicroRNA signatures in human ovarian cancer. Cancer Res **67**(18): 8699-707
- Jakobsen J & Lundbaek K (1976). Neuropathy in experimental diabetes: an animal model. Br Med J **2**(6030): 278-279.
- Jensen MP, Chodroff MJ & Dworkin RH (2007). The impact of neuropathic pain on health-related quality of life: review and implications. Neurology **68**(15): 1178-1182.
- Jain KK (2008). Current challenges and future prospects in management of neuropathic pain. Expert review of Neurotherapeutics **8**(11): 1743-1756.
- Ji RR & Strichartz G (2004). Cell signaling and the genesis of neuropathic pain. Sci STKE **2004**(252): reE14.
- Kim E, Hyrc KL, Speck J, et al. (2010). Regulation of cellular calcium in vestibular supporting cells by Otopetrin 1. J Neurophysiol **104**(6): 3439-3450.
- Kim EH, Ryu DH & Hwang S (2011). The expression of corticotropin-releasing factor and its receptors in the spinal cord and dorsal root ganglion in a rat model of neuropathic pain. Anat Cell Biol **44**: 60-68.
- Kim SH & Chung JM (1992). An experimental model for peripheral neuropathy produced by segmental spinal nerve ligation in the rat. Pain **50**(3): 355-363.
- Krützfeldt J, Rajewsky N, Braich R, et al. (2005). Silencing of microRNAs *in vivo* with 'antagomirs'. Nature **438**: 685-689.
- Kulkarni M, Ozgur S & Stoecklin G (2010). On track with P-bodies. Biochem Soc Trans **38**(1): 242-251.
- Kusuda R, Cadetti F, Ravanelli MI, et al. (2011). Differential expression of microRNAs in mouse pain models. Mol Pain **7**(17).
- Labuz D, Schmidt Y, Schreiter A, et al. (2009) Immune cell-derived opioids protect against neuropathic pain in mice. J Clin Invest **119**: 278.
- Lagos-Quintana M, Rauhut R, Lendeckel W, et al. (2001). identification of novel genes coding for small expressed RNAs. Science **294**(5543): 853-858.
- Lampert A, O'Reilly AO, Reeh P, et al. (2010). Sodium channelopathies and pain. Eur J Physiol **460**: 249-263.
- Langevin SM, Stone RA, Bunker CH, et al. (2011). MicroRNA-137 promoter methylation is associated with poorer overall survival in patients with squamous cell carcinoma of the head and neck. Cancer **117**(7): 1454-1462.
- Lawson SN (1979). The postnatal development of large light and small dark neurons in mouse dorsal root ganglia - a statistical analysis of cell numbers and size. J Neurocytol. **8**(3): 275-294.
- Lee RC, Feinbaum RL & Ambros V (1993). The *C. elegans* heterochronic gene *lin-4* encodes small RNAs with antisense complementarity to *lin-14*. Cell **75**(5): 843-854.
- Lesage F & Lazdunski M (2000). Molecular and functional properties of two-pore-domain potassium channels. Am J Renal Physiol **279**: 793-801.
- Lewis BP, Burge CB & Bartel DP (2005). Conserved seed pairing, often flanked by adenosines, indicates that thousands of human genes are microRNA targets. Cell

- 120(1):** 15-20.
- Liang Z, Zhou H, He Z, et al. (2011a). mirAct: a web tool for evaluating microRNA activity based on gene expression data. *Nucleic Acids Res.* **39**: W139-144.
- Liang Z, Zhou H, Zheng H, et al. (2011b). Expression levels of microRNAs are not associated with their regulatory activities. *Biology Direct.* **6**(43).
- Ma W & Bisby MA (1997). Differential expression of galanin immunoreactivities in the primary sensory neurons following partial and complete sciatic nerve injuries. *Neuroscience* **79**(4): 1183-1195.
- Makeyev EV, Zhang J, Carrasco MA, et al. (2007). The MicroRNA miR-124 promotes neuronal differentiation by triggering brain-specific alternative pre-mRNA splicing. *Molecular Cell* **27**: 435-448.
- Marchand F, Perretti M & McMahon SB (2005). Role of the immune system in chronic pain. *Nat Rev Neurosci* **6**(7): 521-532.
- McCoy CE (2011). The role of miRNAs in cytokine signaling. *Front Biosci* **16**: 2161-2171.
- Merskey H & Bogduk N (Eds). Classification of chronic pain: Descriptions of chronic pain syndromes and definitions of pain terms (1994). IASP Press.
- Moalem G & Tracey DJ (2006). Immune and inflammatory mechanisms in neuropathic pain. *Brain Res Rev* **51**(2): 240-264.
- Mousa SA, Bopaiah CP, Richter JF, et al. (2007) Inhibition of inflammatory pain by Crf at peripheral, spinal and supraspinal sites: Involvement of areas coexpressing Crf receptors and opioid peptides. *Neuropsychopharmacology* **32**(12):2530-42
- Ng KY, Wong YH & Wise H (2010). The role of glial cells in influencing neurite extension by dorsal root ganglion cells. *Neuron Glia Biology* **6**(1): 19-29.
- Ocaña M, Candan CM, Cobos EJ et al. (2004). Potassium channels and pain: Present realities and future opportunities. *Eur J Pharmacol* **500**(1): 203-219.
- Ohara PT, Vit JP, Bhargava A, et al. (2009). Gliopathic pain: When satellite glial cells go bad. *Neuroscientist* **15**(5): 450-463.
- Pasquinelli AE, Reinhart BJ, Slack F, et al. (2000). Conservation of the sequence and temporal expression of let-7 heterochronic regulatory RNA. *Nature* **403**(6772): 901-906.
- Petersen CP, Bordeleau ME, Pelletier J, et al. (2006). Short RNAs repress translation after initiation in mammalian cells. *Mol Cell* **21**: 533-542.
- Pillai RS, Bhattacharyya SN & Filipowicz W (2007). Repression of protein synthesis by miRNAs: how many mechanisms? *Trends Cell Biol* **17**(3): 118-126.
- Ponomarev ED, Veremeyko T, Barteneva N, et al. (2011). MicroRNA-124 promotes microglia quiescence and suppresses EAE by deactivating macrophages via the C/EBP-a-PU.1 pathway. *Nat Med* **17**(1): 64-71.
- Rigaud M, Gemes G, Barabas ME, et al. (2007). Species and strain differences in rodent sciatic nerve anatomy: Implications for studies of neuropathic pain. *Pain* **136**: 188–201
- Reinhold AK, Batti L, Bilbao D, Rittner HL, Heppenstall PA (2014). Differential transcriptional profiling of damaged and intact adjacent dorsal root ganglia neurons in neuropathic pain. (submitted)
- Rolke R, Baron R, Maier C, et al. (2006). Quantitative sensory testing in the German Research Network on neuropathic pain (DFNS): Standardized protocol and reference values. *Pain* **123**(3): 231-243.
- Rose K, Ooi L, Dalle C, et al. (2011). Transcriptional repression of the M channel

- subunit Kv7.2 in chronic nerve injury. *Pain* **152**(4): 742-754.
- Sarantopoulos C, McCallum B, Kwok WM, et al. (2002). Gabapentin decreases membrane calcium currents in injured as well as in control mammalian primary afferent neurons. *Reg Anesth Pain Med* **27**(1): 47-57.
- Sacheli R, Nguyen L, Borgs L, et al. (2009). Expression patterns of miR-96, miR-182 and miR-183 in the developing inner ear. *Gene Expression Patterns* **9**: 364-370.
- Sakai A., Suzuki H. (2013). Nerve injury-induced upregulation of miR-21 in the primary sensory neurons contributes to neuropathic pain in rats. *Biochem. Biophys. Res. Commun* **435**: 176–181
- Schäfers M, Geis C, Svensson CI, et al. (2003). Selective increase of tumour necrosis factor-alpha in injured and spared myelinated primary afferents after chronic constrictive injury of rat sciatic nerve. *Eur J Neurosci* **17**(4): 791-804.
- Schaible HG & Richter F (2004). Pathophysiology of pain. *Langenbecks Arch Surg* **389**(4): 237-243.
- Scholz J & Woolf CJ (2007). The neuropathic pain triad: neurons, immune cells and glia. *Nat Neurosci* **10**(11): 1361-1368.
- Schwenk J, Metz M, Zolles G, et al. (2010). Native GABA(B) receptors are heteromultimers with a family of auxiliary subunits. *Nature* **465**: 231-237.
- Shi TS, Tandrup T, Bergman E, et al. (2001). Effect of peripheral nerve injury on dorsal root ganglion neurons in the C57/6J mouse: marked changes both in cell numbers and neuropeptide expression. *Neuroscience* **105**(1): 249-263.
- Silber J, Lim DA, Petritsch C, et al. (2008). miR-124 and -137 inhibit proliferation of glioblastoma multiforme cells and induce differentiation of brain tumor stem cells. *BMC Medicine* **6**(14).
- Skofitsch G, Zamir N, Helke CJ, et al. (1985). Corticotropin releasing factor-like immunoreactivity in sensory ganglia and capsaicin sensitive neurons of the rat central nervous system: Colocalization with other neuropeptides. *Peptides* **6**: 307-318.
- Smrt RD, Szulwach KE, Pfeiffer RL, et al. (2010). MicroRNA miR-137 regulates neuronal maturation by targeting ubiquitin ligase mind bomb-1. *Stem Cells* **28**(6): 1060-1070.
- Soreq H & Wolf Y (2011). NeurimmiRs: microRNAs in the neuroimmune interface. *Trends Mol Med* **17**(10): 548-555.
- Staaaf S, Oerther S, Lucas G, et al. (2009). Differential regulation of TRP channels in a rat model of neuropathic pain. *Pain* **114**: 187-199.
- Strickland IT, Richards L, Holmes FE, et al. (2011) Axotomy-induced miR-21 promotes axon growth in adult dorsal root ganglion neurons. *PLoS One* **6**(8): e23423.
- Stucky CL & Lewin GR (1999). Isolectin B4-positive and -negative nociceptors are functionally distinct. *J Neurosci* **19**(15): 6497-6505.
- Thulangisam S, Massilamany C, Gangaplar A, et al. (2011). miR-27b*, an oxidative stress-responsive microRNA modulated nuclear factor-kB pathway in RAW 264.7 cells. *Mol Cell Biochem* **352**(1-2): 181-188.
- Toth C, Lander J & Wiebe S (2009). The prevalence and impact of chronic pain with neuropathic pain symptoms in the general population. *Pain Med* **10**(5): 918-9.
- Treede RD, Jensen TS, Campbell JN, et al. (2008). Neuropathic pain: redefinition and a grading system for clinical and research purposes. *Neurology* **70**(18): 1630-5.
- Tronnier VM & Rasche D (2009). Neuroablative procedures in pain therapy. *Schmerz* **23**(5): 531-541.

- Tsujino H, Kondo E, Fukuoka T, et al. (2000). Activating transcription factor 3 (ATF3) induction by axotomy in sensory and motoneurons: A novel neuronal marker of nerve injury. *Mol Cell Neurosci* **15**(2): 170-182.
- Urbich C, Kuehbacher A & Dimmeler S (2008). Role of microRNAs in vasculare diseases, inflammation, and angiogenesis. *Cardiovasc Res* **79**(4): 581-588.
- van der Ree MH, de Bruijne J, Kootstra NA, et al. (2014). MicroRNAs: role and therapeutic target sin viral hepatitis. *Antivir Ther* (epub ahead of print)
- van Dongen S, Abreu-Goodger C & Enright AJ (2008). Detecting microRNA binding and siRNA off-target effects from expression data. *Nat Methods* **5**(12): 1023-1025.
- van Steenwinckel J, Reaux-Le Goazigo A, Pommier B, et al. (2011). CCL2 Released from neuronal synaptic vesicles in the spinal cord is a major mediator of local inflammation and pain after peripheral nerve injury. *J Neurosci* **31**(15): 5865-5875.
- Vasudevan S, Tong Y & Steitz JA (2007). Switching from repression to activation: microRNAs can up-regulate translation. *Science* **318**(5858): 1931-1934.
- Vidal-Sanz M, Villegas-Perez MP, Bray GM, et al. (1988). Persistent retrograde labelling of adult rat retinal ganglion cells with the carbocyanine dye diI. *Exp Neurol* **102**(1): 92-101.
- Villar M, Corté R, Theodorsson E, et al. (1989). Neuropeptide expression in rat dorsal root ganglion cells and spinal cord after peripheral nerve injury with special reference to galanin. *Neuroscience* **33**(3): 587-604.
- Wall PD, Waxman S & Basbaum AI (1974). Ongoing activity in peripheral nerve: injury discharge. *Exp Neurol* **45**(3): 576-589.
- Waselle L, Quaglia X, Zurn AD (2009). Differential proteoglycan expression in two spinal cord regions after dorsal root injury. *Mol Cell Neurosci* **42**(4): 315-27.
- Whitwam JG (1976). Classification of peripheral nerves. *Anaesthesia* **31**(4): 494-503.
- Wood JN, Boorman JP, Okuse K, et al. (2004). Voltage-gated sodium channels and pain pathways. *J Neurobiol* **61**(1): 55-71.
- Woolf CJ & Mannion RJ (1999). Neuropathic pain: aetiology, symptoms, mechanisms, and management. *Lancet* **353**(9168): 1959-1964.
- Xu S, Witmer PD, Lumayag S, et al. (2007). MicroRNA transcriptome of mouse retina and identification of a sensory organ-specific miRNA cluster. *J Biol Chem* **282**(34): 25053-25066.
- Yu B, Zhou S, Qian T, et al. (2011). Altered microRNA expression following sciatic nerve resection in dorsal root ganglia of rats. *Acta Biochim Biophys Sin* **43**(11): 909-915.
- Yuan H, Xu S, Wang Y, Xu H, et al. (2010) Corticotrophin-Releasing Hormone (Crh) facilitates axon outgrowth. *Spinal Cord* **48**: 850.
- Zhao J, Lee MC, Momin A, et al. (2010). Small RNAs control sodium channel expression, nociceptor excitability, and pain thresholds. *J Neurosci* **30**(32): 10860-10871.
- Zheng JH, Walters ET & Song XJ (1007). Dissociation of Dorsal Root Ganglion neurons induces hyperexcitability that it maintained by increased responsiveness to cAMP and cGMP. *J Neurophysiol* **97**: 15-25.
- Zhu M, Yi M, Kim CH, et al. (2011). Integrated miRNA and mRNA expression profiling of mouse mammary tumor models identifies miRNA signatures associated with mammary tumor lineage. *Genome Biol* **12**(8): R77.

8 List of Figures & Tables

- Figure 1.** Principles of nociception
- Figure 2.** Regulatory pathways in injured and non-injured neurons
- Figure 3.** Principles of miRNA biogenesis and action
- Figure 4.** Principle of fluorescent tracer injection
- Figure 5.** Galanin expression in ipsi- and contralateral DRG
- Figure 6.** Condition-based cluster analysis of Luminex data
- Figure 7.** Expression of miR-183 and -137
- Figure 8.** Expression of miR-124, -505, and -27b
- Figure 9.** Chromogenic staining of miR-183 and -137.
- Figure 10.** Fluorescent in-situ hybridisation of naïve DRG for miR-137
- Figure 11.** Representative example of flow cytometry.
- Figure 12.** Microarray similarity analysis
- Figure 13.** Principal Component Analysis on microarray
- Figure 14.** *SylArray* graph of wording regulation in damaged vs contralateral DRG neurons (significant seeds)
- Figure 15.** *SylArray* graph of wording regulation in damaged vs contralateral DRG neurons (candidates)
- Figure 16.** *SylArray* graph of wording regulation in damaged vs adjacent DRG neurons (significant seeds)
- Figure 17.** *SylArray* graph of wording regulation in damaged vs adjacent DRG neurons (candidates)
- Figure 18.** *MirAct* box plot of miRNAs with likely involvement
- Figure 19.** *MirAct* box plot for miR-137, -183, and -124
-
- Table 1.** Exemplary aetiologies of central and peripheral neuropathic pain
- Table 2.** Tracer combinations and their interpretation
- Table 3.** miRNA downregulation 7 d after CCI
- Table 4.** miRNA upregulation 7 d after CCI
- Table 5.** Top putative target genes for miR-183
- Table 6.** Top putative target genes for miR-137
- Table 7.** Group differences (microarray)
- Table 8.** Genes upregulated in damaged DRG neurons compared to contralateral control
- Table 9.** Genes downregulated in damaged DRG neurons compared to contralateral control
- Table 10.** Genes upregulated in damaged DRG neurons compared to adjacent neurons
- Table 11.** Genes downregulated in damaged DRG neurons compared to adjacent neurons
- Table 12.** *MirAct* analysis of gene expression results (most significant)
- Table 13.** *MirAct* analysis of gene expression results (candidates)

9 Abbreviations

5-HT	5-Hydroxytryptamine (serotonin)
Ago2	Argonaute protein
ATP	Adenotriphosphate
CaMK	Ca ²⁺ /calmodulin-dependent protein kinase
CCI	Chronic constriction injury
cDNA	CopyDNA
CGRP	Calcitonin gene-related peptide
CNS	Central nervous system
Ct	Cycle threshold
DIG	Digoxigenin
DiI	1,1-dioctadecyl-3,3,3,3-tetramethylindocarbocyanine perchlorate
DMEM	Dulbecco's Modified Eagle Medium
DMSO	Dimethyl sulfoxide
DNA	Desoxyribonucleic acid
DRG	Dorsal root ganglion
EDTA	Ethylenediaminetetraacetic acid
EL	Expression level
ERK	Extracellular signal-regulated kinase
F-ISH	Fluorescence <i>in situ</i> hybridization
FE	Fluoroemerald
FITC	Fluorescein isothiocyanate
GDNF	Glial cell-derived neurotrophic factor
GIRK	G protein-activated rectifying K ⁺ channels
GPCR	G protein-coupled receptor

IHC	Immunohistochemistry
IL	Interleukin
ISH	<i>In situ</i> hybridization
LNA	Locked nucleic acids
miRNA	MicroRNA
miRNP	MicroRNA ribonuclein complex
mRNA	Messenger RNA
n.s.	Non-significant
NGF	Nerve growth factor
NO	Nitric oxide
nt	Nucleotide
PBS	Phosphate buffered saline
PCA	Principal component analysis
PCR	Polymerase chain reaction
PFA	Para-formaldehyde
PGE ₂	Prostaglandin E ₂
PKA	Protein kinase A
PKC	Protein kinase C
PNS	Peripheral nervous system
qPCR	Quantitative PCR
RISC	RNA-induced silencing complex
RNA	Ribonucleic acid
ROS	Reactive oxygen species
RT	Room temperature
rt-PCR	Reverse-transcription PCR

SNL	Spinal nerve ligation
SSC	Saline-sodium citrate
TEA	Triethanoleamine
TG	Trigeminal ganglion
TNF- α	Tumor necrosis factor α
TrkA	Tyrosine kinase A
tRNA	Transfer RNA
TRP	Transient receptor potential
TTX	Tetradotoxin
UTR	Untranslated region
VIP	Vasoactive intestinal peptide

Danksagung

Dass aus diesem Projekt eine Dissertation entstehen konnte, ist vielen Leuten zu verdanken. Es war eine spannende Zeit, manchmal nervenaufreibend, immer intensiv.

Ich danke meiner Doktormutter, Prof. Dr. med. Heike Rittner, sehr herzlich für ihre Bereitschaft, die Betreuung meiner Dissertation zu übernehmen, mich zu unterstützen und so offen in ihrer Arbeitsgruppe aufzunehmen.

Nichts wäre möglich gewesen ohne Prof. Dr. Paul Heppenstall am EMBL in Monterotondo, der mir dieses spannende Forschungsthema anbot. „There is just one problem – you’d have to go to Rome“... Vielen Dank für diese einmalige Chance, die tolle, produktive und offene Atmosphäre im Labor und die stete Bereitschaft, weitere Ideen auszutüfteln, doch noch einen neuen Ansatz mitzutragen, nicht nachzulassen... Die Zeit am EMBL hat auch mein Verständnis von Wissenschaft entscheidend geprägt, mich gelehrt, Forschung nicht nur methodisch, sondern auch ethisch kritisch zu hinterfragen, und öfter „the big picture“ zu suchen.

In Monterotondo haben mir viele Leute den Start in die Forschung sehr erleichtert. In der AG Heppenstall waren dies vor allem Sandra Zurborg und Brian Yurgionas, die mich mit Expertise, Geduld und Freundschaft den Laboralltag, Techniken und Frustrationstoleranz gelehrt haben.

Ohne Kasper Rasmussen wäre die Welt der microRNA wohl kaum so anschaulich geworden; Daniel „the FACS man“ Bilbao Cortez und Emerald Perlas, der mit großer Expertise und Freundlichkeit in jeglichen Histologiefragen weiterhalf, waren jederzeit Stützen. Weiterhin danke ich Daniele Hasler für die Weiterführung der Färbungen und die Überlassung seiner Aufnahmen für diese Arbeit.

Tausend Dank an meine Eltern und Freunde, die ich als konstante Begleiter stets zur Seite wusste, in Frustrationsphasen wie in Euphoriemomenten.

Grazie, Roma!

Curriculum Vitae

Persönliche Daten

Name: Ann-Kristin Reinhold
Geburtsdatum: 20.08.1983 in Münster (D)

Schullaufbahn

1990 - 1994 Grundschule
1994 - 2003 Friedrichs-Gymnasium Herford
2003 Abitur

Studium

2003 - 2004 European Studies (B.A.), Universiteit Maastricht (NL)
2004 - 2005 Psychologie (Dipl.), Albert-Ludwigs-Universität Freiburg
i. Br.
2005 - 2007 Humanmedizin (StEx), Vorklinischer Abschnitt, Albert-
Ludwigs-Universität Freiburg i. Br.
09 / 2007 Erster Teil der Medizinischen Prüfung
2007 - 2012 Humanmedizin (StEx), Klinischer Abschnitt, Charité
Universitätsmedizin Berlin
05 / 2012 Zweiter Teil der Medizinischen Prüfung, Approbation

Klinische Ausbildung

09 / 2008 Famulatur in der Medizinischen Klinik des Mathilden-
Hospitals Herford
08 / 2009 Famulatur in der Medizinischen Rettungsstelle des
Klinikums am Urban Berlin
03 / 2010 Famulatur in der Pädiatrie im Hospital Universitario de los
Andes Merida (Venezuela)
09 / 2010 Famulatur in Neurozentrum und Anästhesiologie des

Klinikums Frankfurt/Oder

02 – 12 / 2011

Praktisches Jahr des Medizinstudiums

1. Terial Neurologie (Wahlfach) Klinikum E. v. Bergmann (Potsdam),
Prof. Dr. W. Christe
2. Terial Innere Medizin Klinikum E. v. Bergmann (Potsdam)
Prof. Dr. F.X. Kleber (Kardiologie)
Prof. Dr. T. Weinke (Gastroenterologie)
3. Terial Chirurgie Vivantes Klinikum Neukölln (Berlin),
Prof. Dr. S. Eggeling(Thoraxchirurgie),
Prof. Dr. B. Böhm (Viszeralchirurgie)
Prof. Dr. R.-A. Laun (Unfallchirurgie)
Prof. Dr. B. Tillig (Kinderchirurgie)

01 / 2013

Hospitation in der Zentralen Notaufnahme des Queen Elizabeth Central Hospital, Blantyre (Malawi)

seit 05/2013

Assistenzärztin in der Weiterbildung, Klinik und Poliklinik für Anästhesiologie (Prof. Dr. Dr. h.c. N. Roewer)

Wissenschaftliche Ausbildung

2005 – 07

Stud. Hilfskraft am Institut für Allgemeine Psychologie der Albert-Ludwigs-Universität Freiburg (Prof. H. Spada).

seit 2008

Promotionsprojekt“miRNA-Veränderungen bei neuropathischem Schmerz”
(Prof. P. Heppenstall, European Molecular Biology Laboratories (EMBL)/Charité; Prof. H. Rittner)

10 / 2008 – 04 / 09

Trainee am EMBL Montorotondo im Rahmen der Promotion (Prof. P. Heppenstall).

05 – 11 / 2009

Stud. Hilfskraft am Neurowissenschaftlichen Forschungszentrums Berlin (Prof. F. Zipp).

12 / 2010 – 02 / 11

Visiting Scientist am EMBL Montorotondo im Rahmen der Promotion (Prof. P. Heppenstall)

10 / 2012 – 01 / 13

Wissenschaftliche Mitarbeiterin der Klinik für Neurologie, TU München. Projekt *Neurological side effects associated with neurocysticercosis following mass drug administration for the control of schistosomiasis in Malawi* (Dr. Dr. A. Winkler)

seit 05/2013

Mitarbeiterin der AG “Molekulare Schmerzforschung”, Klinik für Anästhesiologie (Prof. Rittner/Prof. Brack)

Förderungen/Stipendien

2004 – 12 Stipendiatin der *Studienstiftung des Deutschen Volkes*

2007 – 08 Kollegiatin des *Studienkollegs zu Berlin*.

Sprachkenntnisse

Englisch: fließend in Sprache und Schrift

Spanisch: fließend in Sprache und Schrift

Italienisch: Konversationsniveau

Französisch, Niederländisch: Grundkenntnisse